Introduction to Theoretical Nuclear Physics

Tetsuo Hyodo

August 4, 2026

Abstract

Lecture notes of Introduction to Theoretical Nuclear Physics for the 2026 academic year. Some parts have been updated from the original version used in class, so equation numbers and other references may differ.

Contents

1 Introduction: hadrons, resonances, and entanglement

1.1 Hadrons and QCD

- **Hadrons**: particles that interact via the strong interaction
- Fundamental theory of the strong interaction: **QCD**

$$\mathcal{L}_{\mathrm{QCD}} = -\frac{1}{4} G^a_{\mu\nu} G^{\mu\nu a} + \bar{q}(i\not{D} - m_q)q. \tag{1}$$

  SU(3) color gauge theory of quarks and gluons

- Observed hadrons [1]
  - qqq baryons $(p, n, \Lambda, \cdots)$: about 170 states
  - $q\bar{q}$ mesons $(\pi, K, \eta, \cdots)$: about 210 states
- Quarks have three colors: r, g, b.
  All observed hadrons are color singlets (color-neutral states).
  No explicit constraint in QCD forbids colored states.
  → Problem of **color confinement**
- Quarks have six flavors: u, d, s, c, b, t.
  Flavor quantum numbers of conventional hadrons are described by qqq or $q\bar{q}$.
  No explicit constraint in QCD forbids multiquark configurations such as $\bar{q}\bar{q}qq$, $\bar{q}qqqq$, $\cdots$.
  → Problem of **exotic hadrons**

1.2 Exotic hadrons and resonances

- Recent observations of exotic hadron candidates [2, 3]
  Only ~ 10 candidates out of ~ 380 hadrons
- Pentaquark candidates $P_c(4312), P_c(4440), P_c(4457)$ [4, 5] (Fig. 1, left)

$$P_c \to J/\psi(\bar{c}c) + p(uud). \tag{2}$$

  Minimal quark content[1]: $\bar{c}cuud$

- Tetraquark candidate T_{cc} [6, 7] (Fig. 1, right)

$$T_{cc} \to D^0(\bar{u}c)D^{*+}(\bar{d}c) \to D^0 D^0 \pi^+. \tag{3}$$

  Minimal quark content: $cc\bar{u}\bar{d}$

[1] In principle, P_c could be described by uud, but it is highly unnatural to explain their masses without a $\bar{c}c$ pair.

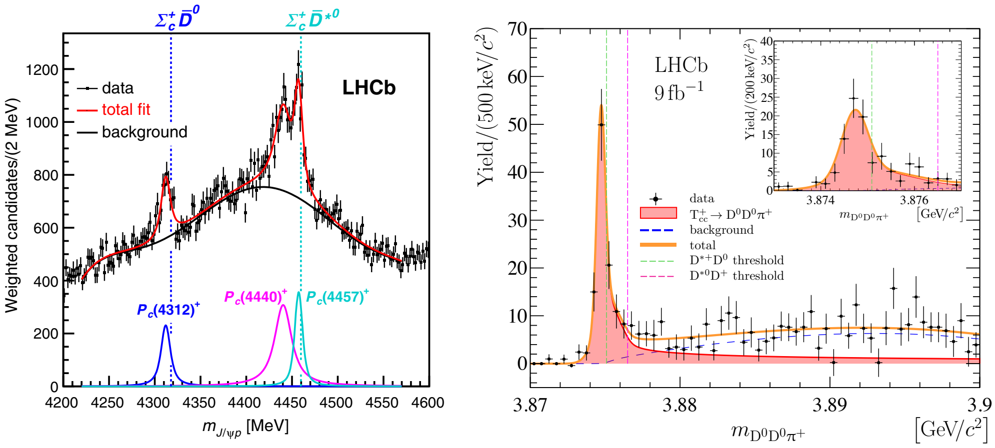

Figure 1: Examples of exotic hadron candidates. Left: spectrum of the pentaquark candidates P_c, adapted from R. Aaij *et al.* (LHCb collaboration), Phys. Rev. Lett. **122**, 222001 (2019). Right: spectrum of the tetraquark candidate T_{cc}, adapted from R. Aaij *et al.* (LHCb collaboration), Nature Phys. **18**, 751 (2022).

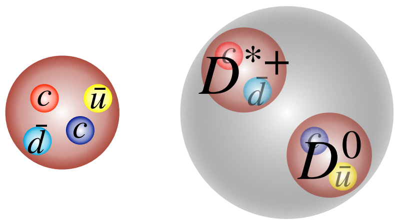

Figure 2: Schematic illustration of a multiquark state (left) and a hadronic molecule (right).

- Exotic hadrons are observed in the spectra of decay products,

$$P_c \to J/\psi + p, \tag{4}$$

$$T_{cc} \to D^0 + D^0 + \pi^+. \tag{5}$$

  Unstable states → treated as **resonances** in hadron scattering
  In fact, only ∼ 20 out of ∼ 380 hadrons are stable.

- Various possible internal structures
  - Multiquarks: compact color-singlet states
    $cc\bar{u}\bar{d}$ for T_{cc} (Fig. 2, left)
  - Hadronic molecules: weakly bound states of hadrons
    $D^0 D^{*+}$ for T_{cc} (Fig. 2, right)

- States with the same quantum numbers can mix with each other:

$$|T_{cc}\rangle = c_1 |cc\bar{u}\bar{d}\rangle + c_2 |D^0 D^{*+}\rangle + \cdots . \tag{6}$$

  How can we determine the weights c_i?
  Is such a decomposition well-defined?
  What is a resonance "state" $|T_{cc}\rangle$?

- Plan of the first half of this lecture
  - §2 (21 April): Resonances $\leftrightarrow$ eigenstates with complex energies
  - §3 (28 April): Definition of the scattering amplitude
  - §4 (12 May): Resonances $\leftrightarrow$ poles of the scattering amplitude
  - §5 (19 May): Feshbach resonances (bound states embedded in the continuum)
  - §6 (26 May): Nonrelativistic effective field theory
  - §7 (9 June): Compositeness and weak-binding relation

1.3 Hadron scattering and quantum entanglement

- Study of hadron scattering
  - Important for extracting resonance information
  - Provides basic information on hadronic molecules
- Prototype of hadron scattering: **nuclear force** (nucleon–nucleon scattering)
- Nucleons have internal degrees of freedom: **spin** and **isospin**
  - Spin $S = 1/2$: $|\uparrow\rangle\,,\ |\downarrow\rangle$
  - Isospin $I = 1/2$: $|p\rangle\,,\ |n\rangle$
- Two-nucleon states: combinations of spin and isospin
  Many possible scattering channels: $|p\uparrow p\uparrow\rangle\,, |p\uparrow n\downarrow\rangle\,, \cdots$
- Symmetry in QCD: $\mathrm{SU}(2)_S \times \mathrm{SU}(2)_I$
  The interaction is invariant under independent rotations of spin and isospin.
  Some processes are forbidden, and different processes are related to each other.
  $\to$ Scattering can be described with a small number of independent components.
- Low-energy s-wave scattering can be described by only **two channels**.

- $^1S_0$ ($S = 0$, $I = 1$)
- $^3S_1$ ($S = 1$, $I = 0$)

These channels are independent of each other.

- Empirical properties of nuclear forces
  - Similar behavior in the $S = 0$ and $S = 1$ channels
    Spin-flavor SU(4) symmetry [8, 9]
  - Large scattering lengths (near the unitary limit)
    Nonrelativistic conformal symmetry [10]

$\rightarrow$ Suggestive of **emergent symmetries** beyond QCD

- Quantum entanglement in two-spin systems
  - Product state: no correlation between spins

$$|\uparrow\downarrow\rangle = |\uparrow\rangle \otimes |\downarrow\rangle \,. \tag{7}$$

  - Entangled state (Bell state): correlated spins

$$|S = 0\rangle = \frac{|\uparrow\downarrow\rangle - |\downarrow\uparrow\rangle}{\sqrt{2}}. \tag{8}$$

- **Entanglement entropy (EE)**
  A quantitative measure of quantum correlation
- Scattering as a quantum operation
  The scattering matrix S acts on the initial state:

$$|\mathrm{out}\rangle = S\,|\mathrm{in}\rangle \,. \tag{9}$$

  S can generate entanglement between nucleons.
- **Entanglement suppression** [11]
  Condition: scattering does not generate entanglement.
  $\rightarrow$ Constraints on scattering amplitudes
  $\rightarrow$ Explanation of **emergent symmetries** in nuclear forces
- Plan of the second half of this lecture
  - §8 (16 June): Spin-1/2 states

- §9 (23 June): Entanglement entropy
- §10 (30 June): Classical and quantum correlations
- §11 (7 July): Bell's inequality
- §12 (14 July): Entanglement power of the S matrix
- §13 (21 July): Nuclear forces and entanglement suppression
- §14 (28 July): Generalization to spin and flavor

1.4 References

- Resonances in quantum mechanics
  Textbook : 羽田野-井村 [12], A. Bohm [13], N. Moiseyev [14]
  Review article : Ashida-Gong-Ueda [15]

- Scattering theory
  Textbook : J.R. Taylor [16], R.G. Newton [17], 永江-兵藤 [18]
  Review article : Hyodo-Niiyama [19]

- Exotic hadrons and compositeness
  Review article : T. Hyodo [20], Kinugawa-Hyodo [21]
  物理学会誌：兵藤哲雄 [22]
  数理科学：兵藤哲雄 [23]

- Quantum information science
  Textbook : 石坂-小川-河内-木村-林 [24], Nielsen-Chuang [25]
  Review article : Robin-Savage [26]

2 Resonances in quantum mechanics

2.1 Overview of resonance states

- **Resonance**: a quantum-mechanically formed metastable "**state**" that decays over time
- Decay products are scattering states (continuum). $\to$ **scattering theory**
  Example: $T_{cc} \to D^0 D^{*+} \Leftrightarrow T_{cc}$ is a resonance in the $D^0 D^{*+}$ scattering.
- Inelastic scattering and channels
  - Elastic scattering: initial state = final state ($D^0 D^{*+} \to D^0 D^{*+}$, ...)
  - Inelastic scattering: transitions to different final states ($D^0 D^{*+} \to D^{*0} D^{*+}$, ...)
  - Channels: multi-body states specified by their particle content ($D^0 D^{*+}$, $D^{*0} D^{*+}$, ...)
- Various characterizations of resonances: how are they related?
  - Peak in cross sections: Fig. 3(a)
  - $\pi/2$ crossing of the phase shift $\delta(E)$: Fig. 3(b)
  - **Pole** of the scattering amplitude in the complex energy plane: Fig. 3(c)
  - **Eigenstate** of the Hamiltonian with **complex** energy: Fig. 3(d)

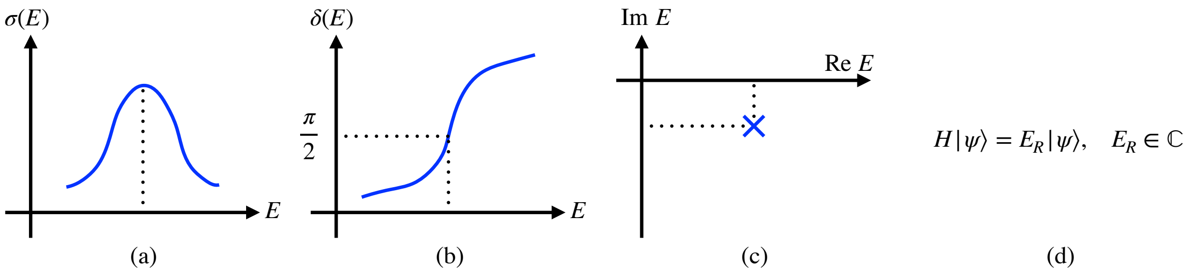

Figure 3: Schematic characterization of resonances. (a) Peak in the total cross section $\sigma(E)$, (b) $\pi/2$ crossing of the phase shift $\delta(E)$, (c) pole of the scattering amplitude, (d) complex eigenenergy.

- **Shape resonance** (potential resonance): Fig. 4(b)
  - Single-channel scattering
    Typical potential: short-range attraction plus a repulsive barrier
  - Energy $E > 0$
  - Unstable due to tunneling

- **Feshbach resonance**: Fig. 4(c)
  - Coupled-channel scattering
    P: entrance channel, Q: closed channel
  - Threshold of Q at $E = \Delta > 0$, threshold of P at $E = 0$
  - A bound state in channel Q at $0 < E < \Delta$
  - Unstable via the $Q \to P$ transition

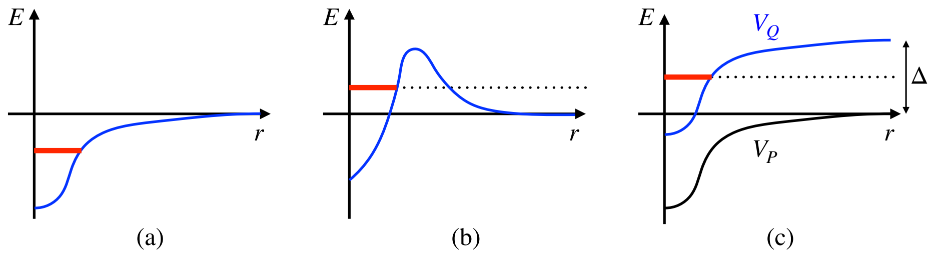

Figure 4: Illustration of a bound state (a), shape resonance (b), and Feshbach resonance (c).

2.2 Resonances as eigenstates of Hamiltonian

- α decay of atomic nuclei: Gamow introduced a **complex eigenenergy** [27],

$$E = M_R - \frac{i\Gamma_R}{2}. \tag{10}$$

- Time evolution of the wave function ($\hbar = 1$)

$$\Psi(t) \propto \exp\{-iEt\} = \exp\{-iM_R t\} \exp\{-\Gamma_R t/2\}. \tag{11}$$

  Probability decreases exponentially, $|\Psi(t)|^2 \propto \exp\{-\Gamma_R t\}$.

- Inconsistent with "expectation value of Hamiltonian H (hermitian operator) is real"?
  $\leftarrow$ Space on which the operator acts [domain $D(H)$] needs to be specified.
  - Eigenvalues are real if $D(H)$ is Hilbert space (square-integrable functions $L^2(\mathbb{R}^d)$)

$$\int |\Psi(x)|^2 dx < \infty. \tag{12}$$

  - Example of a non-square-integrable wave function: plane wave $\Psi(x) \sim e^{\pm ipx}$

$$\int_{-\infty}^{\infty} |\Psi(x)|^2 dx = \int_{-\infty}^{\infty} 1 \; dx \to \infty. \tag{13}$$

- Can we find an eigenstate with complex E?

2.3 Square-well potential

- Schrödinger equation

$$\left(-\frac{1}{2\mu}\frac{d^2}{dr^2}+V(r)\right)u_0(r)=Eu_0(r), \quad 0\le r\le\infty. \tag{14}$$

$u_0(r)\sim$ radial wave function of spherical 3D potential with $\ell=0$: $\psi_{\ell,m}(\boldsymbol{r})=\dfrac{u_\ell(r)}{r}Y_\ell^m(\hat{\boldsymbol{r}})$

- Attractive square-well potential ($V_0>0$)

$$V(r)=\begin{cases}-V_0 & 0\le r\le b\\ 0 & b<r\end{cases}. \tag{15}$$

- General solutions (without boundary conditions)

$$u_0(r)\propto\begin{cases}e^{\pm ikr} & 0\le r\le b, \quad k=\sqrt{2\mu(E+V_0)}\\ e^{\pm ipr} & b<r, \quad p=\sqrt{2\mu E}\end{cases}. \tag{16}$$

- Scattering solutions (with boundary condition $u_0(r\to 0)=0$)

$$u_0(r)=\begin{cases}C\sin(kr) & 0\le r\le b\\ A^-(p)e^{-ipr}+A^+(p)e^{+ipr} & b<r\end{cases}, \tag{17}$$

$$A^\pm(p)=\frac{C}{2}\left[\sin(kb)\mp i\frac{k}{p}\cos(kb)\right]e^{\mp ipb}. \tag{18}$$

  – Solutions exist for any $E>0$: **continuous** spectrum

  – Scattering solutions are not normalizable (they do not vanish as $r\to\infty$).
  $\to$ Overall normalization C is arbitrary.

  – $A^\pm(p)$ are determined by the continuity of u_0 and du_0/dr at $r=b$.

  – The waves $e^{\pm ipr}$ propagate in the $\pm r$ directions.
  A^+ (A^-) is the amplitude of the outgoing (incoming) wave.

2.4 Discrete eigenstates

- Discrete eigenstates: obtained by imposing boundary conditions both at $r\to 0$ and $r\to\infty$

- Bound state solution: eigenenrgy $E<0\Leftrightarrow$ purely imaginary eigenmomentum $p=\sqrt{2\mu E}$

$$p=i\kappa, \quad \kappa>0. \tag{19}$$

Wave function at $r\to\infty$ behaves as

$$u_0(r)=A^-(i\kappa)e^{+\kappa r}+A^+(i\kappa)e^{-\kappa r} \quad (r\to\infty). \tag{20}$$

Table 1: Numerical solutions for Eq. (22) with $V_0 = 10\mu^{-1}b^{-2}$.

	p $[b^{-1}]$	$E = p^2/(2\mu)$ $[\mu^{-1}b^{-2}]$
Bound state B	$+3.68i$	-6.78
1st resonance R_1	$1.06 - 1.02i$	$0.05 - 1.08i$
2nd resonance R_2	$6.29 - 1.41i$	$18.8 - 8.86i$
3rd resonance R_3	$9.90 - 1.69i$	$47.6 - 16.8i$
$\vdots$		

- Boundary condition: square integrable $u_0(r) \to$ eliminate the diverging component $e^{+\kappa r}$

$$A^-(i\kappa) = 0. \tag{21}$$

For $p = i\kappa$, the incoming wave (e^{-ipr}) vanishes, leaving only the outgoing wave (e^{+ipr}).

- $A^-(p) = 0$: **Outgoing (Siegert) boundary condition**

$$\tan(\sqrt{p^2 + 2\mu V_0}\ b) = -i\frac{\sqrt{p^2 + 2\mu V_0}}{p}. \tag{22}$$

Substituting $p = i\kappa$, the well-known bound-state condition $\kappa = -k\cot(kb)$ is recovered.

- Bound states: solution of Eq. (22) with pure imaginary p
$\leftrightarrow$ Physical scattering occurs for real and positive p.
$\Rightarrow$ Bound state solution is obtained by **analytic continuation** of Eq. (22).

- Resonance states: solutions of Eq. (22) with **complex** p

- Attractive square well potential has infinitely many resonance solutions [28, 14].
Table 1: numerical solutions of Eq. (22) with $V_0 = 10\mu^{-1}b^{-2}$
Poles of $1/A^-(p)$ in complex p plane (Fig. 5, left)

- Imaginary part of eigenmomentum is negative,

$$p = p_R - ip_I, \quad p_R, p_I > 0. \tag{23}$$

Behavior of wave function

$$u_0(r) \to A^+(p)e^{ipr} \propto \underbrace{e^{ip_R r}}_{\text{oscillation}}\ \underbrace{e^{+p_I r}}_{\text{increasing}}. \tag{24}$$

$u_0(r)$ diverges with oscillation for $r \to \infty$ and is **not square integrable** (Fig. 5, right).

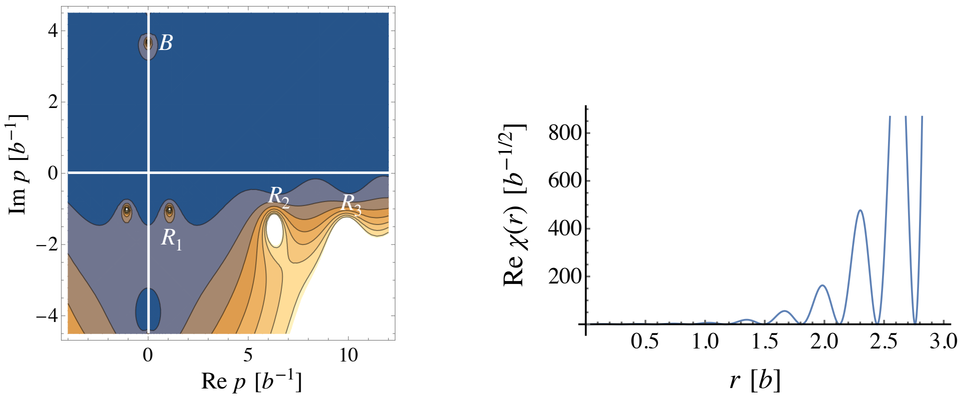

Figure 5: Left: contour plot of $1/|A^{-}(p)|$ of square well potential (15) with $V_0 = 10\mu^{-1}b^{-2}$. Right: real part of wave function of the third resonance R_3.

2.5 Summary of §2

- Discrete eigenstates ← outgoing boundary condition
- Resonances: eigenstates of the Hamiltonian with complex eigenenergy
  Analogous to bound states (analytic continuation of eigenmomentum)
- Resonance wave functions diverge as $r \to \infty$ (complex p).

3 Scattering theory primer

3.1 Preliminaries

- Simple setup
  - Quantum scattering of distinguishable particles 1, 2 (mass m_1, m_2)
  - Hamiltonian $H = H_0 + V$ (H_0 : kinetic term, V : potential)
  - Nonrelativistic system in three spatial dimensions
  - No internal degrees of freedom (spin, flavor, etc.)
  - Elastic scattering (initial state = final state, no coupled channels)
  - Rotational symmetry $\Leftrightarrow$ spherical potential $V(r) \Leftrightarrow [H, \boldsymbol{L}] = \boldsymbol{0}$
  - Short-range interaction [$V(r)$ vanishes at $r \to \infty$ sufficiently rapidly]

- Kinematics $\leftarrow$ relative momentum (Fig. 6)
  - Initial state: $\boldsymbol{p}$ [in CM frame, particle 1 (2) has momentum $\boldsymbol{p}$ ($-\boldsymbol{p}$)]
  - Final state: $\boldsymbol{p}'$

  Elastic scattering $\to$ magnitude is unchanged: $p \equiv |\boldsymbol{p}| = |\boldsymbol{p}'|$

- **Two** parameters which characterize the scattering process
  - Scattering angle θ

    $$\cos\theta = \frac{\boldsymbol{p}\cdot\boldsymbol{p}'}{p^2}. \tag{25}$$

  - Scattering energy E (or momentum p)

    $$E = \frac{p^2}{2\mu}, \tag{26}$$

    with the reduced mass $\mu = m_1 m_2/(m_1 + m_2)$

- Physical scattering occurs for $E > 0$, $p > 0$[2]

- Wave function $\leftarrow$ time-independent Schrödinger equation for energy E (§2)

[2]For physical scattering, either E or p can be used. However, for analytic continuation to the complex plane, the S matrix and the scattering amplitude introduced below should be regarded as meromorphic functions of p.

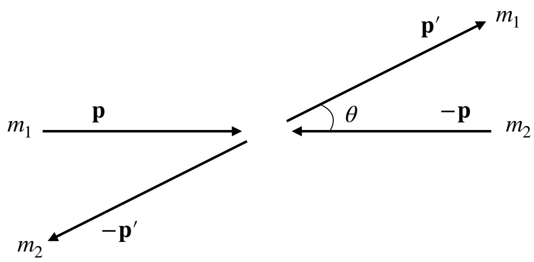

Figure 6: Schematic illustration of the kinematics of the scattering.

- Initial state $|\boldsymbol{p}\rangle$ and final state $\langle\boldsymbol{p}'|$: eigenstates of H_0 with the normalization

$$\langle\boldsymbol{p}'|\boldsymbol{p}\rangle = \delta^3(\boldsymbol{p}'-\boldsymbol{p}), \quad H_0\,|\boldsymbol{p}\rangle = \frac{p^2}{2\mu}\,|\boldsymbol{p}\rangle\,. \tag{27}$$

  With the normalization $1 = \int d\boldsymbol{r}\,|\boldsymbol{r}\rangle\,\langle\boldsymbol{r}|$, the wave function is $\langle\boldsymbol{r}|\boldsymbol{p}\rangle = e^{i\boldsymbol{p}\cdot\boldsymbol{r}}/(2\pi)^{3/2}$.

- Angular momentum representation: initial $|E,\ell,m\rangle$, final $\langle E',\ell',m'|$

$$\langle E',\ell',m'|E,\ell,m\rangle = \delta(E'-E)\delta_{\ell'\ell}\delta_{m'm}. \tag{28}$$

- Relation between two vectors:

$$\langle\boldsymbol{p}'|E,\ell,m\rangle = \frac{1}{\sqrt{\mu p}}\delta\left(\frac{(p')^2}{2\mu}-E\right)Y_\ell^m(\hat{\boldsymbol{p}}'). \tag{29}$$

3.2 Scattering amplitude

- Scattering operator: transition from initial state to final state

$$\mathsf{S} = \Omega_-^\dagger\Omega_+ = \lim_{t\to+\infty}[e^{iH_0t}e^{-iHt}]\lim_{t\to-\infty}[e^{iHt}e^{-iH_0t}]. \tag{30}$$

  $\Omega_\pm$: Møller operators

- ***S*-matrix** element (also called S matrix): $s_\ell(E)\in\mathbb{C}$

$$\langle E',\ell',m'|\,\mathsf{S}\,|E,\ell,m\rangle = \delta(E'-E)\delta_{\ell'\ell}\delta_{m'm}s_\ell(E). \tag{31}$$

- **Phase shift**: $\delta_\ell(E)\in\mathbb{R}$

$$s_\ell(E) = \exp\{2i\delta_\ell(E)\}. \tag{32}$$

- ***T* matrix**: $t(\boldsymbol{p}'\leftarrow\boldsymbol{p})\in\mathbb{C}$

$$\langle\boldsymbol{p}'|\,(\mathsf{S}-1)\,|\boldsymbol{p}\rangle = -2\pi i\delta(E'-E)t(\boldsymbol{p}'\leftarrow\boldsymbol{p}). \tag{33}$$

- **Scattering amplitude**: $f(E,\theta) \in \mathbb{C}$ (with the present convention)

$$f(E,\theta) = -(2\pi)^2\mu\, t(\boldsymbol{p}' \leftarrow \boldsymbol{p})$$
$$= \sum_{\ell=0}^{\infty}(2\ell+1)f_\ell(E)P_\ell(\cos\theta) \quad \text{(partial wave decomposition)}. \tag{34}$$

Relation to S matrix

$$f_\ell(E) = \frac{s_\ell(E)-1}{2ip}. \tag{35}$$

- $s_\ell, \delta_\ell, f_\ell$ are functions of E for each ℓ.

3.3 Unitarity and scattering cross section

- From definition (30), S operator is **unitary** (when H is Hermitian),

$$\mathsf{S}^\dagger\mathsf{S} = 1. \tag{36}$$

Norm (probability) is conserved during time evolution

- From the completeness relation $1 = \int dE \sum_{\ell,m} |E,\ell,m\rangle\langle E,\ell,m|$ and definition (31),

$$s_\ell^*(E)s_\ell(E) = |s_\ell(E)|^2 = 1. \tag{37}$$

This indicates that phase shift is real (when $E > 0$),

$$\exp\{2i(\delta_\ell(E) - \delta_\ell^*(E))\} = 1 \quad \Rightarrow \quad \mathrm{Im}\ \delta_\ell(E) = 0. \tag{38}$$

- Scattering cross section

$$\sigma(E) = \int d\Omega |f(E,\theta)|^2 = \sum_\ell 4\pi(2\ell+1)|f_\ell(E)|^2. \tag{39}$$

Substituting Eq. (35),

$$\sigma(E) = \sum_{\ell=0}^{\infty}\sigma_\ell(E), \tag{40}$$

$$\sigma_\ell(E) = \frac{2\pi(2\ell+1)}{\mu E}\sin^2\delta_\ell(E). \tag{41}$$

- **Unitarity bound**: Since $\sin^2\delta_\ell(E) \le 1$, cross section has an upper bound (Fig. 7),

$$\sigma_\ell(E) \le \frac{2\pi(2\ell+1)}{\mu E}. \tag{42}$$

The equality holds when $\sin\delta_\ell = \pm 1$, namely, $\delta_\ell = \dfrac{\pi}{2}$ (modulo π).

- For $E \to 0$, the upper bound of $\sigma_\ell(E)$ diverges (unitarity limit).

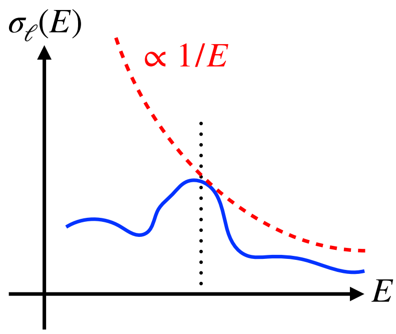

Figure 7: Schematic figure of cross section. Dashed line shows the unitarity bound $2\pi(2\ell+1)/(\mu E)$.

3.4 Jost functions

- **Riccati functions**
  - 3D wave function $\psi_{\ell,m}(\boldsymbol{r})$ with $V=0$ ($p=\sqrt{2\mu E}$):

$$\psi_{\ell,m}(\boldsymbol{r}) = [Aj_\ell(pr) + Bn_\ell(pr)]Y_\ell^m(\hat{\boldsymbol{r}}) = [Ch_\ell^-(pr) + Dh_\ell^+(pr)]Y_\ell^m(\hat{\boldsymbol{r}}). \tag{43}$$

    $j_\ell(z)$ [$n_\ell(z)$]: spherical Bessel (Neumann) function, $h_\ell^\pm(z)$: spherical Hankel functions[3]

  - Riccati-Bessel/Neumann function: useful to expand radial wave function $u_\ell(r) \propto r\psi_{\ell,m}(\boldsymbol{r})$

$$\hat{j}_\ell(z) = zj_\ell(z), \quad \hat{n}_\ell(z) = zn_\ell(z). \tag{44}$$

  - Riccati-Hankel functions

$$\hat{h}_\ell^\pm(z) = zh_\ell^\pm(z) \to \exp\{\pm i(z-\ell\pi/2)\} \quad (z\to\infty). \tag{45}$$

    Thus, $\hat{h}_\ell^+(pr) \sim e^{+ipr}$ [$\hat{h}_\ell^-(pr) \sim e^{-ipr}$] is **outgoing (incoming)** wave.

- **Regular solution** $\phi_{\ell,p}(r)$: $u_\ell(r)$ with eigenmomentum p normalized as

$$\frac{\phi_{\ell,p}(r)}{\hat{j}_\ell(pr)} \to 1 \quad (r\to 0). \tag{46}$$

  Together with $\phi_{\ell,p}(r)\to 0$ at $r=0$, this fixes the normalization (derivative).

- Asymptotic form of $\phi_{\ell,p}(r)$ at $r\to\infty$: superposition of Riccati functions because of $V=0$

$$\phi_{\ell,p}(r) \to \frac{i}{2}\left[\not{f}_\ell(p)\hat{h}_\ell^-(pr) - [\not{f}_\ell(p)]^*\hat{h}_\ell^+(pr)\right] \quad (r\to\infty). \tag{47}$$

  Since the radial Schrödinger equation does not contain i and the slope at the origin is real, $\phi_{\ell,p}(r)$ is **real**. $\Rightarrow D = C^*$ $\left([\hat{h}^\pm(z)]^* = \hat{h}^\mp(z)\right)$ for $\phi_{\ell,p}(r) = C\hat{h}_\ell^-(pr) + D\hat{h}_\ell^+(pr)$

[3] The definition of the Neumann function often includes a minus sign, e.g., $n_0(z) = -\cos z/z$. In scattering theory, however, the convention $n_0(z) = +\cos z/z$ is frequently used [16].

- **Jost function** $\not{f}_\ell(p)$: coefficient of incoming wave $\leftarrow$ Eq. (45)

$$\not{f}_\ell(p) = 1 + \frac{2\mu}{p}\int_0^\infty dr\, \hat{h}^+_\ell(pr)V(r)\phi_{\ell,p}(r). \tag{48}$$

- **Outgoing boundary condition = zero of Jost function** $\not{f}_\ell(p)$

- Jost function is an analytic function of p ($\sim$ having no singularity)[4].

- Expansion of $\not{f}_\ell(p)$ for small p: shown by integral representation (48)

$$\not{f}_\ell(p) = 1 + \underbrace{[\alpha_\ell + \beta_\ell p^2 + \mathcal{O}(p^4)]}_{\text{even powers of } p} + i\underbrace{[\gamma_\ell p^{2\ell+1} + \mathcal{O}(p^{2\ell+3})]}_{\text{odd powers of } p}, \quad \alpha_\ell, \beta_\ell, \gamma_\ell, \dots \in \mathbb{R}. \tag{49}$$

- Complex conjugate of Jost function $\leftarrow$ Eq. (49)

$$\left[\not{f}_\ell(p)\right]^* = \not{f}_\ell(-p^*). \tag{50}$$

$\Rightarrow$ For physical scattering ($p > 0$),

$$\phi_{\ell,p}(r) \to \frac{i}{2}\left[\not{f}_\ell(p)\hat{h}^-_\ell(pr) - \not{f}_\ell(-p)\hat{h}^+_\ell(pr)\right] \quad (r \to \infty). \tag{51}$$

- s-wave case ($\ell = 0$) : $\hat{j}_0(pr) = \sin(pr)$, $\hat{h}^\pm_0(pr) = e^{\pm ipr}$

- Solution (17) of square-well potential in §2.3

$$u_0(r) \to C\sin(kr) = Ckr + \mathcal{O}(r^3). \tag{52}$$

- Normalization of Eq. (46) : from $\hat{j}_0(pr) = pr + \mathcal{O}(r^3)$

$$\phi_{\ell,p}(r) = u_0(r)\Big|_{C=\frac{p}{k}} \tag{53}$$

- Jost function of square-well potential

$$\frac{i}{2}\not{f}^{\text{well}}_0(p) = A^-(p)\Big|_{C=\frac{p}{k}}$$
$$\not{f}^{\text{well}}_0(p) = \left[\cos(kb) - i\frac{p}{k}\sin(kb)\right]e^{ipb}. \tag{54}$$

This expression follows the expansion (49) for small $p \Rightarrow A^+(p) = -\frac{i}{2}\not{f}_\ell(-p)$ with $C = \frac{p}{k}$.

[4]Strictly speaking, region of analyticity in complex p plane is determined by the behavior of $V(r)$ with Eq. (48).

4 Resonances in scattering theory

4.1 Resonances as poles of scattering amplitude

- Discrete eigenstates of Hamiltonian ← outgoing boundary condition (QM, §2)
- Outgoing boundary condition ← zeros of Jost function $\not{f}_\ell(p) = 0$ (scattering theory, §3)
- S-matrix from wave function: amplitude of outgoing wave normalized by the incoming one

$$u_\ell(r) \to \hat{h}_\ell^-(pr) - s_\ell(p)\hat{h}_\ell^+(pr) \quad (r \to \infty). \tag{55}$$

Comparing with Eq. (51), we find,

$$s_\ell(p) = \frac{\not{f}_\ell(-p)}{\not{f}_\ell(p)}. \tag{56}$$

⇒ Discrete eigenstates are represented by **poles of S-matrix**

- Scattering amplitude: from Eq. (35)

$$f_\ell(p) = \frac{s_\ell(p) - 1}{2ip} = \frac{\not{f}_\ell(-p) - \not{f}_\ell(p)}{2ip\not{f}_\ell(p)}. \tag{57}$$

⇒ Discrete eigenstates are represented by **poles of scattering amplitude**.

- $s_\ell(p)$ and $f_\ell(p)$ are meromorphic functions of p ($\sim$ no singularities except for poles).

4.2 Eigenenergies and Riemann sheets

- Analytic continuation of $\not{f}_\ell(p)$, $s_\ell(p)$, $f_\ell(p)$ defined in physical region $p > 0$ to complex plane
- Complex momentum p and complex energy E

$$p = |p|e^{i\theta_p}, \quad E = |E|e^{i\theta_E}. \tag{58}$$

- Relation between p and E

$$E = \frac{p^2}{2\mu} = \frac{|p|^2}{2\mu}e^{2i\theta_p} \quad \Rightarrow \quad |E| = \frac{|p|^2}{2\mu}, \quad \theta_E = 2\theta_p. \tag{59}$$

  - When θ_p varies $0 \to 2\pi$, θ_E varies $0 \to 4\pi$.
  - p and $-p$ (θ_p and $\theta_p + \pi$) are mapped onto the same value of E.

- Meromorphic functions of p [$s_\ell(p)$, $f_\ell(p)$] are defined on two-sheeted Riemann surface of E.
  $0 \le \theta_E < 2\pi$: first Riemann sheet of E (upper half-plane of p, $0 \le \theta_p < \pi$)
  $2\pi \le \theta_E < 4\pi$: **second Riemann sheet** of E (lower half-plane of p, $\pi \le \theta_p < 2\pi$)

- Fig. 8: Complex p and E planes
  Branch cut along real axis of E plane (branch point at $E = 0$)

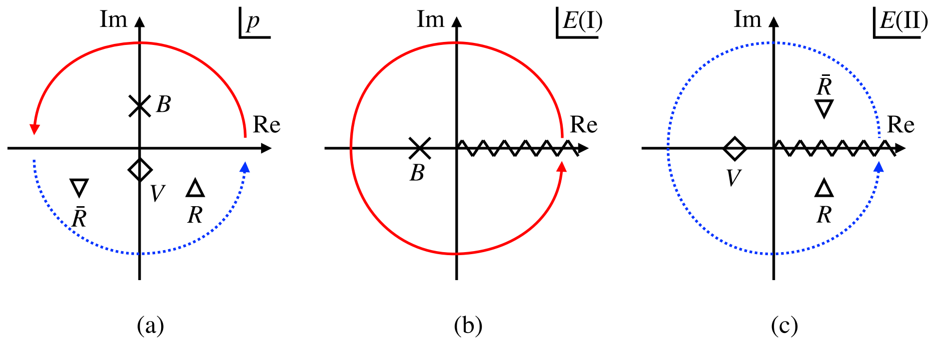

Figure 8: Poles in the complex plane. (a): p plane, (b): E plane (first Riemann sheet), (c): E plane (second Riemann sheet). B, V, R, and $\bar{R}$ represent a bound state, a virtual state, a resonance, and an anti-resonance, respectively.

4.3 Classification of eigenstates

- Eigenstate of Hamiltonian: zero of Jost function $\not{f}_\ell(p) = 0$
- From Eq. (50), if $\not{f}_\ell(p) = 0$,

$$\not{f}_\ell(-p^*) = [\not{f}_\ell(p)]^* = 0. \tag{60}$$

  $\Rightarrow$ If p is a solution, then $-p^*$ is also a solution.

- Solutions with $p = -p^*$ (on the imaginary axis)
  - Bound state (B): $\times$ in Fig. 8

$$\mathrm{Re}\ p_B = 0, \quad \mathrm{Im}\ p_B > 0. \tag{61}$$

    Energy $E_B = p_B^2/(2\mu)$ is real and negative (first Riemann sheet)
  - Virtual state (anti-bound state, V): $\diamondsuit$

$$\mathrm{Re}\ p_V = 0, \quad \mathrm{Im}\ p_V < 0. \tag{62}$$

    The energy $E_V = p_V^2/(2\mu)$ is real and negative (second Riemann sheet).
    The residue of the pole ($\sim$ norm) is negative [29, 30], non-physical degree of freedom?

- Solutions with $p \neq -p^*$ (always appearing in pairs)
  - Exist only in lower half-plane of p
    $\leftarrow$ Complex E is allowed only when wave function is not square-integrable.

- **Resonance** (R): $\triangle$

$$\text{Re } p_R > 0, \quad \text{Im } p_R < 0. \tag{63}$$

Re $E_R > 0$, Im $E_R < 0$ (second Riemann sheet)

- Anti-resonance $(\bar{R})$: $\triangledown$

$$\text{Re } p_{\bar{R}} < 0, \quad \text{Im } p_{\bar{R}} < 0. \tag{64}$$

Appears together with resonance
A solution growing in time [31] ("conjugate" of the resonance)

4.4 Resonances and observables

- Only real energies are experimentally accessible.
  Effect of a resonance pole at $E = E_R = M_R - i\Gamma_R/2$ on observables in partial wave ℓ

- $f_\ell(E)$ having a pole at $E = E_R$:

$$f_\ell(E) = f_{\ell,\text{BW}}(E) + f_{\ell,\text{BG}}(E). \tag{65}$$

Breit-Wigner term $f_{\ell,\text{BW}}(E)$: resonance contribution

$$f_{\ell,\text{BW}}(E) = \frac{-\Gamma_R}{2p}\frac{1}{E - E_R} = \frac{-\Gamma_R}{2p}\frac{E - M_R - i\Gamma_R/2}{(E - M_R)^2 + \Gamma_R^2/4}. \tag{66}$$

Nonresonant background $f_{\ell,\text{BG}}(E)$: analytic at $E = E_R$ and slowly varying

- At real $E \sim M_R$, contribution from $f_{\ell,\text{BW}}(E)$ increases (in particular, for narrow Γ_R).

- When $f_{\ell,\text{BG}}(E)$ is **assumed** to be small and negligible,

$$f_\ell(E) \approx f_{\ell,\text{BW}}(E) \quad (f_{\ell,\text{BG}}(E) \approx 0). \tag{67}$$

we observe a "resonance" at **real energy** $E = M_R$:

(i) Re $f_\ell(E) = 0$ and Im $f_\ell(E)$ becomes maximal (Fig. 9) $\leftarrow$ Eq. (66)

(ii) Cross section $\sigma(E)$ exhibits a peak $\leftarrow$ (i) and the optical theorem (Exercise 2)

(iii) Phase shift $\delta_\ell(E)$ increases rapidly and crosses $\pi/2$.
$\leftarrow$ From Eq. (35), Im $s_\ell(M_R) = 0$ when Re $f_\ell(M_R) = 0$.
$\leftarrow$ Except for $\delta_\ell = 0$ (non-interacting case), we have $\delta_\ell = \pi/2$ (modulo π)

- When $f_{\ell,\text{BG}}(E)$ is non-negligible, interference term contributes,

$$|f_\ell(E)|^2 = |f_{\ell,\text{BW}}(E)|^2 + |f_{\ell,\text{BG}}(E)|^2 + 2\text{Re}\left[f_{\ell,\text{BW}}(E)f^*_{\ell,\text{BG}}(E)\right]. \tag{68}$$

Peaks can be generated kinematically without a pole (e.g. threshold cusps) [32],
$\Rightarrow$ Importance of a careful analysis to determine resonance poles

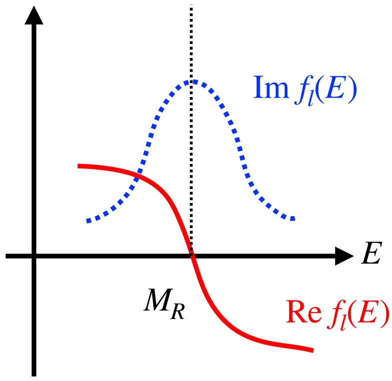

Figure 9: Schematic illustration of scattering amplitude near the resonance energy M_R.

4.5 Effective range expansion

- Low-energy (small p) behavior of scattering amplitude $f_\ell(p)$

$$f_\ell(p) = \frac{s_\ell(p)-1}{2ip} = \frac{1}{p\cot\delta_\ell(p) - ip} = \frac{p^{2\ell}}{p^{2\ell+1}\cot\delta_\ell(p) - ip^{2\ell+1}}. \tag{69}$$

- From Eq. (49), Jost function can be written as,

$$\not{f}_\ell(p) = F_\ell(p^2) + ip\,G_\ell(p^2) \quad \Leftrightarrow \quad \not{f}_\ell(-p) = F_\ell(p^2) - ip\,G_\ell(p^2). \tag{70}$$

F_ℓ and G_ℓ are functions of p^2 and behave as $(p\to 0)$,

$$F_\ell(p^2) = \mathcal{O}(p^0), \quad G_\ell(p^2) = \mathcal{O}(p^{2\ell}). \tag{71}$$

- From Eq. (57)

$$f_\ell(p) = \frac{\not{f}_\ell(-p) - \not{f}_\ell(p)}{2ip\not{f}_\ell(p)} = \frac{p^{2\ell}}{-p^{2\ell}F_\ell(p^2)/G_\ell(p^2) - ip^{2\ell+1}}. \tag{72}$$

- Comparing Eqs. (69) and (72), we obtain,

$$p^{2\ell+1}\cot\delta_\ell(p) = -p^{2\ell}\frac{F_\ell(p^2)}{G_\ell(p^2)}. \tag{73}$$

Right-hand side is a function of p^2 with $\mathcal{O}(p^0)$ as $p\to 0$, and its Taylor expansion reads

$$\Rightarrow \quad p^{2\ell+1}\cot\delta_\ell(p) = -\frac{1}{a_\ell} + \frac{r_\ell}{2}p^2 + \mathcal{O}(p^4), \tag{74}$$

which is called the **effective range expansion**.

- s-wave case ($\ell = 0$)

$$f_0(p) = \frac{1}{-\frac{1}{a_0} + \frac{r_0}{2}p^2 + \mathcal{O}(p^4) - ip}. \tag{75}$$

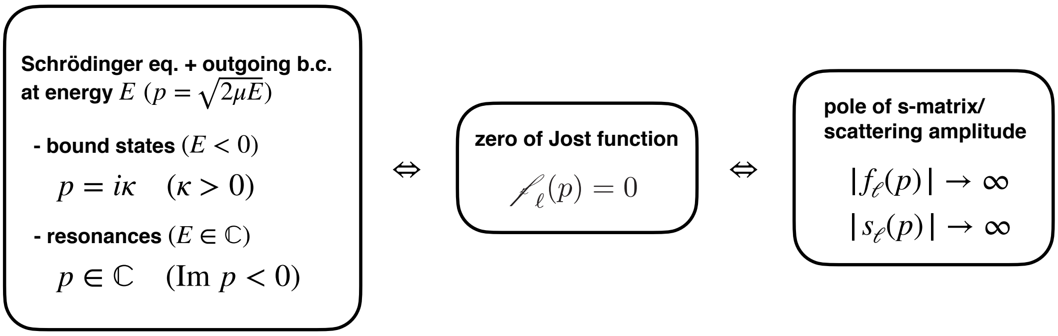

Figure 10: Various conditions for resonances. The outgoing boundary condition of the wave function is related to the poles of the scattering amplitude through the zeros of the Jost function.

- $a_0 \equiv a$: scattering length (opposite sign convention is also used in hadron physics).
- r_0: effective range, roughly corresponds to the interaction range, but can be negative.
- Eq. (73) can have poles (CDD poles [33]).
  When a CDD pole exists at low energy, Padé approximant is useful [34, 35].

- Low-energy scattering: assuming higher-order terms in p are negligible,

$$f_0(p) \approx \frac{1}{-\frac{1}{a} - ip} \tag{76}$$

  Pole at $p = \dfrac{i}{a}$

  - $a > 0$: pole in the upper half-plane $\Rightarrow$ bound state ($E = -1/(2\mu a_0^2) < 0$)
  - $a < 0$: pole in the lower half-plane $\Rightarrow$ virtual state ($E = -1/(2\mu a_0^2) < 0$)
  - $a \to \pm\infty$: pole at $p = 0$ ($E = 0$, **unitary limit**)

4.6 Summary of §3 and §4

- Definitions of S-matrix, phase shift, scattering amplitude, etc.
- Correspondence between poles of scattering amplitude and resonance states (Fig. 10)
- Effective range expansion: description of low-energy scattering

5 Theory of Feshbach resonances

5.1 Introduction

- Feshbach resonance: a resonance in **coupled-channel** scattering
- Threshold energy $E_{\rm th}$ and channels at energy E
  - Open channels ($E > E_{\rm th}$): scattering occurs
  - Closed channels ($E < E_{\rm th}$): no scattering occurs
- Original work: theory of compound nuclear reactions [36, 37] (Fig. 11, left)
- Cold atoms experiments: control of scattering length by a magnetic field [38] (Fig. 11, right)

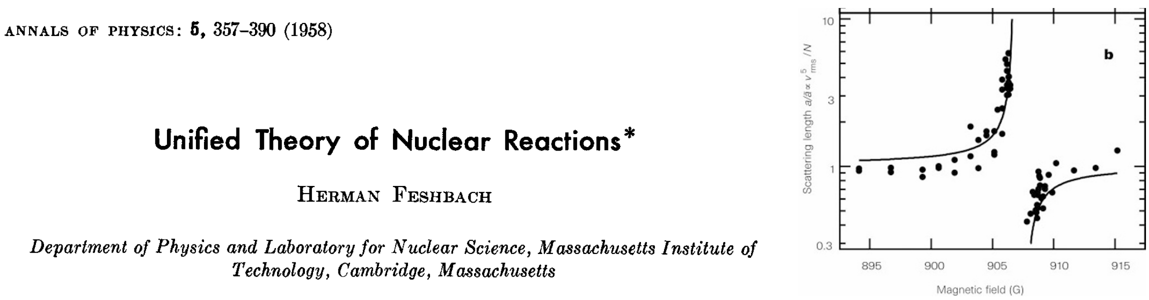
ANNALS OF PHYSICS: **5**, 357–390 (1958)

Unified Theory of Nuclear Reactions*

HERMAN FESHBACH

Department of Physics and Laboratory for Nuclear Science, Massachusetts Institute of Technology, Cambridge, Massachusetts

Figure 11: Left: H. Feshbach, Ann. Phys. **5**, 357 (1958). Right: Control of the scattering length in cold atoms by a magnetic field, adopted from S. Inouye, Nature (London) **392**, 151 (1998).

5.2 Two-channel Hamiltonian

- Two channels P and Q, with the threshold of P set at $E_{\rm th}(P) = 0$ [39]
- Schrödinger equation in matrix form (a set of equations)

$$\hat{H}\,|\psi\rangle = E\,|\psi\rangle\,, \tag{77}$$

$$\hat{H} = \begin{pmatrix} \hat{H}_{PP} & \hat{H}_{PQ} \\ \hat{H}_{QP} & \hat{H}_{QQ} \end{pmatrix} = \begin{pmatrix} \dfrac{\hat{\boldsymbol{p}}^2}{2\mu_P} + \hat{V}_P & \hat{V}_t \\ \hat{V}_t & \dfrac{\hat{\boldsymbol{p}}^2}{2\mu_Q} + \Delta + \hat{V}_Q \end{pmatrix}, \quad |\psi\rangle = \begin{pmatrix} |P\rangle \\ |Q\rangle \end{pmatrix}. \tag{78}$$

  - $\hat{V}_P, \hat{V}_Q$: potentials in each channel (Fig. 4), vanishing at $r \to \infty$
  - $\hat{V}_t$: channel-transition potential

- $\Delta = E_{\text{th}}(Q) - E_{\text{th}}(P) > 0$ (originating from the Zeeman splitting $\propto$ magnetic field)
- For $0 < E < \Delta$, P is open and Q is closed.

- Projection operators

$$\hat{P} = \begin{pmatrix} 1 & 0 \\ 0 & 0 \end{pmatrix}, \quad \hat{Q} = \begin{pmatrix} 0 & 0 \\ 0 & 1 \end{pmatrix}, \tag{79}$$

$$\hat{P}^2 = \hat{P}, \quad \hat{Q}^2 = \hat{Q}, \quad \hat{P}\hat{Q} = \hat{Q}\hat{P} = 0, \quad \hat{P} + \hat{Q} = \hat{I}. \tag{80}$$

Each component of $|\psi\rangle$ or $\hat{H}$ can be written as $|X\rangle = \hat{X}\,|\psi\rangle$ and $\hat{H}_{XY} = \hat{X}\hat{H}\hat{Y}$.

- **Effective Hamiltonian for channel P** $\leftarrow$ eliminating $|Q\rangle$

Lower component of Eq. (77)

$$\begin{aligned} \hat{H}_{QP}\,|P\rangle + \hat{H}_{QQ}\,|Q\rangle &= E\,|Q\rangle \\ \hat{H}_{QP}\,|P\rangle &= (E - \hat{H}_{QQ})\,|Q\rangle \\ |Q\rangle &= (E - \hat{H}_{QQ})^{-1}\hat{H}_{QP}\,|P\rangle \,. \end{aligned} \tag{81}$$

Upper component of Eq. (77)

$$\hat{H}_{PP}\,|P\rangle + \hat{H}_{PQ}\,|Q\rangle = E\,|P\rangle$$

$$\hat{H}_{PP}\,|P\rangle + \hat{H}_{PQ}(E - \hat{H}_{QQ})^{-1}\hat{H}_{QP}\,|P\rangle = E\,|P\rangle$$

$$\Rightarrow \quad \hat{H}^{\text{eff}}(E)\,|P\rangle = E\,|P\rangle \,, \tag{82}$$

$$\hat{H}^{\text{eff}}(E) = \hat{H}_{PP} + \hat{H}_{PQ}(E - \hat{H}_{QQ})^{-1}\hat{H}_{QP}. \tag{83}$$

$\hat{H}^{\text{eff}}(E)$ effectively incorporates the effect of Q.

- Single-channel (not in matrix form) Schrödinger equation for P
- No approximations $\Rightarrow$ Solution of Eq. (82) is equivalent to $|P\rangle$ in Eq. (77).
- $\hat{H}^{\text{eff}}(E)$ is energy dependent $\rightarrow$ Self-consistent solutions for discrete eigenstates

5.3 Single-resonance approximation

- Eigenstates of $\hat{H}_{QQ}$ without the transition ($\hat{V}_t = 0$, $\hat{V}_Q \neq 0$, see Fig. 12):

$$\hat{H}_{QQ}\,|\phi_i\rangle = \epsilon_i\,|\phi_i\rangle \quad \text{(bound states)}, \tag{84}$$

$$\hat{H}_{QQ}\,|\phi(\epsilon)\rangle = \epsilon\,|\phi(\epsilon)\rangle \quad \text{(continuum states labeled by energy } \epsilon\text{)}. \tag{85}$$

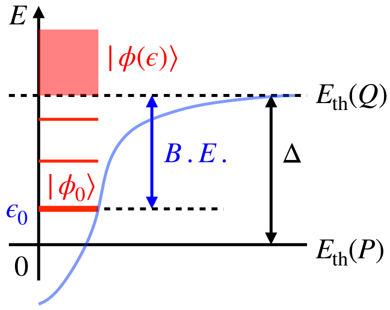

Figure 12: Schematic illustration of the eigenstates of $\hat{H}_{QQ}$.

- Spectral decomposition (continuum starts from $\epsilon = \Delta$)

$$\hat{I} = \sum_i |\phi_i\rangle \langle\phi_i| + \int_\Delta^\infty d\epsilon\, |\phi(\epsilon)\rangle \langle\phi(\epsilon)| , \tag{86}$$

$$\hat{H}^{\rm eff}(E) = \frac{\hat{\boldsymbol{p}}^2}{2\mu_P} + \hat{V}_P + \sum_i \frac{\hat{H}_{PQ} |\phi_i\rangle \langle\phi_i| \hat{H}_{QP}}{E - \epsilon_i} + \int_\Delta^\infty d\epsilon \frac{\hat{H}_{PQ} |\phi(\epsilon)\rangle \langle\phi(\epsilon)| \hat{H}_{QP}}{E - \epsilon + i0^+} . \tag{87}$$

- $\hat{H}^{\rm eff}(E)$ acquires an imaginary part for $E > \Delta$,

$$\int dx \frac{f(x)}{x - a + i0^+} = \mathcal{P} \int dx \frac{f(x)}{x - a} - i\pi f(a) \quad \text{(if } a \in \text{integration range).} \tag{88}$$

- When $|\epsilon_0|$ is sufficiently small, the dominant contribution for $E \ll \Delta$ is,

$$\hat{H}^{\rm eff}(E) \approx \frac{\hat{\boldsymbol{p}}^2}{2\mu_P} + \frac{\hat{V}_t |\phi_0\rangle \langle\phi_0| \hat{V}_t}{E - \epsilon_0} . \tag{89}$$

- ϵ_0 is measured from $E_{\rm th}(P) = 0$; binding energy $(B.E.)$ from $E_{\rm th}(Q) = \Delta$ is,

$$B.E. = \Delta - \epsilon_0 . \tag{90}$$

  $B.E.$ is fixed by $\hat{H}_{QQ}$ $\Rightarrow$ If Δ is proportional to magnetic field, ϵ_0 can be tuned.

5.4 Scattering amplitude and resonance

- $\hat{H}^{\rm eff}$ is a single-channel Hamiltonian for P $\Rightarrow$ Scattering theory in §3 can be applied.

$$\hat{H}^{\rm eff} = \hat{H}_0 + \hat{V}, \quad \hat{H}_0 = \frac{\hat{\boldsymbol{p}}^2}{2\mu_P}, \quad \hat{V} = \frac{\hat{V}_t |\phi_0\rangle \langle\phi_0| \hat{V}_t}{E - \epsilon_0}, \quad \hat{H}_0 |\boldsymbol{p}\rangle = \frac{\boldsymbol{p}^2}{2\mu_P} |\boldsymbol{p}\rangle . \tag{91}$$

- **Lippmann–Schwinger (LS) equation** for the wave function $|P\rangle$

$$|P\rangle = |\boldsymbol{p}\rangle + \hat{G}\hat{V} |P\rangle . \tag{92}$$

  Free Green's operator (resolvent)

$$\hat{G}(E) = (E - \hat{H}_0)^{-1} . \tag{93}$$

- T operator and scattering amplitude

$$\hat{T} = \hat{V} + \hat{V}\hat{G}\hat{T} = \hat{V} + \hat{V}\hat{G}\hat{V} + \hat{V}\hat{G}\hat{V}\hat{G}\hat{V} + \cdots, \tag{94}$$

$$\langle \boldsymbol{p}'|\,\hat{T}(E+i0^+)\,|\boldsymbol{p}\rangle = t(\boldsymbol{p}' \leftarrow \boldsymbol{p}) = -\frac{1}{(2\pi)^2\mu_P} f(E,\theta), \tag{95}$$

- LS equation for the T matrix (integral equation)

$$t(\boldsymbol{p}' \leftarrow \boldsymbol{p}) = \langle \boldsymbol{p}'|\,\hat{V}\,|\boldsymbol{p}\rangle + \int d\boldsymbol{q}\,\langle \boldsymbol{p}'|\,\hat{V}\,|\boldsymbol{q}\rangle\,\frac{1}{E - \boldsymbol{q}^2/(2\mu_P) + i0^+} t(\boldsymbol{q} \leftarrow \boldsymbol{p}). \tag{96}$$

- The potential $\hat{V}$ in Eq. (91) is **separable** (a product of functions of $\boldsymbol{p}$ and $\boldsymbol{p}'$),

$$\langle \boldsymbol{p}'|\,\hat{V}(E)\,|\boldsymbol{p}\rangle = \frac{\langle \boldsymbol{p}'|\,\hat{V}_t\,|\phi_0\rangle\,\langle\phi_0|\,\hat{V}_t\,|\boldsymbol{p}\rangle}{E - \epsilon_0} = \lambda F^*(\boldsymbol{p}')F(\boldsymbol{p}), \tag{97}$$

$$\lambda = \frac{1}{E-\epsilon_0}, \quad F(\boldsymbol{p}) = \langle\phi_0|\,\hat{V}_t\,|\boldsymbol{p}\rangle \quad \text{(form factor)}. \tag{98}$$

In this case, the scattering amplitude can be written in a closed form,

$$f(E,\theta) = -(2\pi)^2\mu_P \frac{F^*(\boldsymbol{p}')F(\boldsymbol{p})}{\dfrac{1}{\lambda} - \displaystyle\int d\boldsymbol{q}\frac{|F(\boldsymbol{q})|^2}{E - \boldsymbol{q}^2/(2\mu_P) + i0^+}} = \frac{-(2\pi)^2\mu_P F^*(\boldsymbol{p}')F(\boldsymbol{p})}{E - \epsilon_0 - \Sigma(E)}, \tag{99}$$

$$\Sigma(E) = \int d\boldsymbol{q}\frac{|F(\boldsymbol{q})|^2}{E - \boldsymbol{q}^2/(2\mu_P) + i0^+} \quad \text{(self energy)}. \tag{100}$$

- Pole condition:

$$0 = E - \epsilon_0 - \Sigma(E). \tag{101}$$

- When $\hat{V}_t = 0$ (no channel transition), $\Sigma(E) = 0$, and hence

$$E = \epsilon_0 \in \mathbb{R}. \tag{102}$$

$\Rightarrow$ Bound state by $\hat{H}_{QQ}$ (decoupled from channel P)

- When $\hat{V}_t \neq 0$, pole is a solution of $E - \epsilon_0 - \Sigma(E) = 0$ in general.
For weak $\hat{V}_t$, a perturbative approximation gives:

$$E \approx \epsilon_0 + \Sigma(\epsilon_0) \in \mathbb{C} \quad \text{for } \epsilon_0 > 0. \tag{103}$$

$\Rightarrow$ **Resonance with a complex eigenenergy** in channel P
Bound state of $\hat{H}_{QQ}$ acquires a decay width through coupling to the continuum of P.

5.5 Summary of §5

- Coupled-channel Hamiltonian for P and Q
- Elimination of channel Q to obtain an effective Hamiltonian in P
- A bound state $|\phi_0\rangle$ in Q couples to P and generates a state with complex energy.

6 Nonrelativistic effective field theory

6.1 Effective field theories

- Microscopic quantum field theory $\mathcal{L}_{\text{micro}}$
- Λ: ultraviolet **cutoff** scale (see Fig. 13)
- Effective Field Theory (EFT) $\mathcal{L}_{\text{EFT}}$
  - describes the same phenomena as $\mathcal{L}_{\text{micro}}$ up to Λ, and
  - can be constructed systematically.

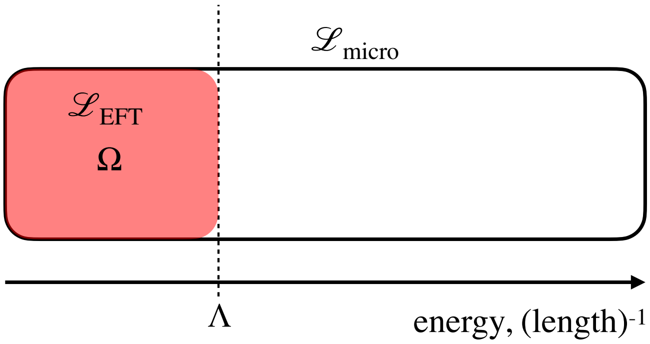

Figure 13: Schematic illustration of effective field theory.

- Electromagnetic interaction
  - Microscopic theory: QED
    Photons ($m_\gamma = 0$), electrons ($m_e \neq 0$)
  - EFT: **Euler-Heisenberg theory** [40]
    Only photons, "heavy" electrons are integrated out ($\Lambda \sim m_e$)
- Weak interaction
  - Microscopic theory: Weinberg-Salam theory
    Leptons, neutrinos, $W^\pm, Z$
  - EFT: **Fermi theory** (Fig. 14)
    Only leptons and neutrinos, "heavy" bosons are integrated out ($\Lambda \sim m_{W^\pm}, m_Z$)
    $W^\pm, Z$ exchange $\rightarrow$ Contact four-Fermi interaction (Fig. 14)

$$\text{Interaction} \propto \frac{g_w^2}{q^2 - m_W^2} = -\frac{g_w^2}{m_W^2}\left(1 + \mathcal{O}\left(\frac{q^2}{m_W^2}\right)\right). \tag{104}$$

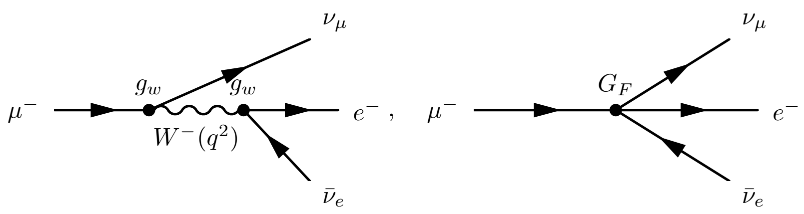

Figure 14: Schematic figure of μ^- decay. Left: Weinberg–Salam theory; Right: Fermi theory.

- Strong interaction
  - Microscopic theory: QCD
    Low-energy d.o.f. (hadrons) are **different** from microscopic d.o.f. (quarks and gluons).
  - Weinberg's "theorem" [41]
    The **most general** $\mathcal{L}_{\text{EFT}}$ consistent with the **symmetries** of $\mathcal{L}_{\text{micro}}$ works.
  - EFT: chiral perturbation theory ← Chiral symmetry of QCD [42]
    Infinitely many terms? → Organized by power counting

$$\mathcal{L}_{\text{ChPT}} = \mathcal{L}^{(\text{LO})} + \mathcal{L}^{(\text{NLO})} + \cdots . \tag{105}$$

6.2 Zero-range model

- EFT for nonrelativistic two-body scattering processes
- R_{typ}: typical length scale of short-range interaction
  - Square well potential: $R_{\text{typ}} = b$ (well width)
  - Yukawa potential $V(r) = g\dfrac{e^{-\kappa r}}{r}$: $R_{\text{typ}} = 1/\kappa$
  - van der Waals potential $V(r) = -\dfrac{C_6}{r^6}$: $R_{\text{typ}} \sim \ell_{\text{vdW}} = \left(\dfrac{mC_6}{\hbar^2}\right)^{1/4}$
- **Zero-range model** $\mathcal{L}_{\text{ZR}}$: s-wave scattering with $|a| \gg R_{\text{typ}}$ [43]

$$f(p) = \frac{1}{-\frac{1}{a} - ip}. \tag{106}$$

  - Nucleons: Yukawa potential due to pion (π) exchange [44]

$$a(^1\text{S}_0) \simeq -23.76 \text{ fm}, \quad a(^3\text{S}_1) \simeq 5.42 \text{ fm}, \quad |a| \gg R_{\text{typ}} \sim \frac{1}{m_\pi} \approx 1.43 \text{ fm}. \tag{107}$$

  - ^{4}He atoms: van der Waals potential due to polarization

$$a \simeq 200 \text{ [Bohr radius]} \qquad |a| \gg R_{\text{typ}} \sim \ell_{\text{vdW}} \sim 10 \text{ [Bohr radius]}. \tag{108}$$

- At low energies $p \ll 1/R_{\rm typ}$, both systems can be described by the same $\mathcal{L}_{\rm ZR}$ (**universality**).
- Lagrangian density of zero-range model

$$\mathcal{L}_{\rm ZR}(t,\boldsymbol{x}) = \underbrace{\psi^\dagger(t,\boldsymbol{x})\left(i\partial_t + \frac{\boldsymbol{\nabla}^2}{2m}\right)\psi}_{\text{kinetic term}} - \underbrace{\frac{\lambda_0}{4}[\psi^\dagger(t,\boldsymbol{x})\psi(t,\boldsymbol{x})]^2}_{\text{interaction term}}, \tag{109}$$

$$\psi(t,\boldsymbol{x}) : \text{bosonic field}, \quad m : \text{boson mass}, \quad \lambda_0 : \text{(bare) coupling constant}. \tag{110}$$

(two fermions with an antisymmetric spin wave function $\sim$ two bosons)

- Quantization: equal-time commutation relations

$$[\psi(t,\boldsymbol{x}),\psi(t,\boldsymbol{x}')] = 0, \quad [\psi(t,\boldsymbol{x}),\psi^\dagger(t,\boldsymbol{x}')] = \delta^3(\boldsymbol{x}-\boldsymbol{x}'). \tag{111}$$

- Interaction term: four-point contact interaction $\sim$ 3d δ function potential

$$-\mathcal{L}_{\rm int} = \frac{\lambda_0}{4}(\psi^\dagger\psi)^2 \sim \mathcal{H}_{\rm int} \sim \text{(energy)}, \tag{112}$$

$$\begin{cases} \lambda_0 > 0 & \text{increase energy} \Rightarrow \text{repulsion} \\ \lambda_0 < 0 & \text{decrease energy} \Rightarrow \text{attraction} \end{cases}. \tag{113}$$

- **Symmetries**: space-time translations, rotations, parity, Galilean boosts, phase symmetry

$$\psi \to e^{i\theta}\psi, \quad N = \int d\boldsymbol{x}\ \psi^\dagger\psi \quad \text{(particle number)}. \tag{114}$$

$\Rightarrow \mathcal{L}_{\rm int}$ does not change the particle number (a two-body state remains a two-body state).

6.3 Feynman rules

- Calculation of physical quantities in quantum field theory

  1. Derive Feynman rules (pieces of Feynman diagrams).
  2. Sum over all possible Feynman diagrams (possible in two-body sector of $\mathcal{L}_{\rm ZR}$).

  2'. Perform perturbation theory (if step 2 is not feasible).

- Propagator: propagation of a particle (Fig. 15, left)

$$G(\omega,\boldsymbol{k}) = \frac{i}{\omega - \boldsymbol{k}^2/(2m) + i0^+}. \tag{115}$$

Only positive-energy component: propagation is forward in time only.

- Vertex: interaction (Fig. 15, middle)

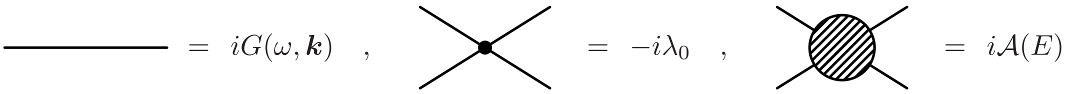

Figure 15: Feynman rules of the zero-range model (109). Left: boson propagator G; Middle: vertex $-i\lambda_0$; Right: four-point function $i\mathcal{A}$.

6.4 Two-boson scattering

- Two-body scattering amplitude $\leftarrow$ four-point function $i\mathcal{A}(E)$ (2 in, 2 out, Fig. 15, right)
- Write down all diagrams from Feynman rules with fixed initial and final states (Fig. 16).

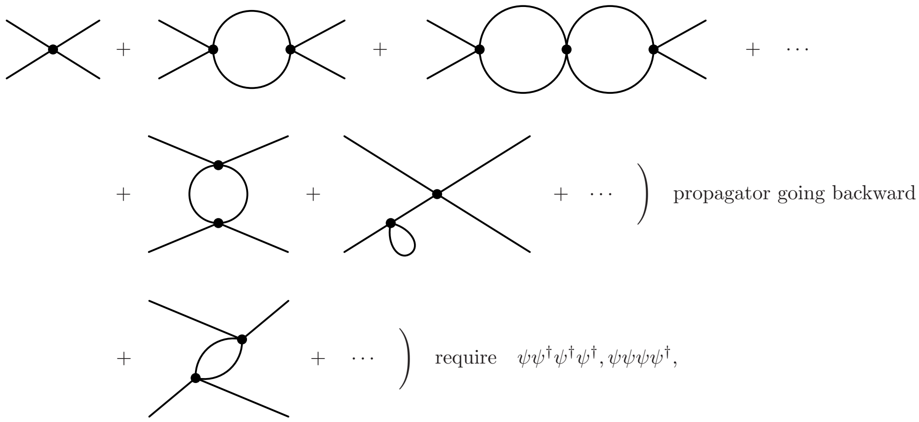

Figure 16: Candidates of Feynman diagrams.

- Eventually, the same structure as the Lippmann–Schwinger equation emerges (Fig. 17).

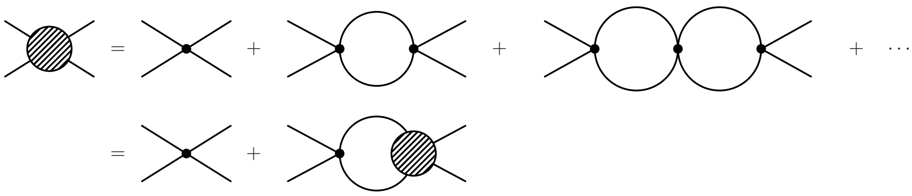

Figure 17: Possible Feynman diagrams.

- Terms of order $(\lambda_0)^n$ are summed to all orders: nonperturbative scattering amplitude.
- Two-body scattering amplitude $\mathcal{A}(E)$

$$i\mathcal{A}(E) = -i\lambda_0 - i\lambda_0 \frac{1}{2} \int \frac{d\omega d\boldsymbol{q}}{(2\pi)^4} G(\omega, \boldsymbol{q}) G(E-\omega, -\boldsymbol{q}) i\mathcal{A}(E). \tag{116}$$

- 1/2: symmetry factor
- Completeness relation in QFT: $1 = \int \frac{d\boldsymbol{q}}{(2\pi)^3} |\boldsymbol{q}\rangle \langle \boldsymbol{q}|$
- dq integration diverges: introduce cutoff Λ (integral range $0 \leq q \leq \Lambda$)
- $i\mathcal{A}(E)$ in r.h.s. is not integrated over $\sim$ Separable interaction in momentum space

- $\mathcal{A}(E)$ can be obtained algebraically,

$$\mathcal{A}(E) = \left[-\frac{1}{\lambda_0} - \frac{m}{4\pi^2} \left(\Lambda - \sqrt{-mE - i0^+} \arctan \frac{\Lambda}{\sqrt{-mE - i0^+}} \right) \right]^{-1}. \tag{117}$$

- Energy E and momentum p

$$E = \frac{p^2}{2\mu} = \frac{p^2}{m} \quad \leftarrow \quad \mu = \frac{mm}{m+m} = \frac{m}{2}. \tag{118}$$

For physical scattering $E > 0$, $p > 0$,

$$\sqrt{-mE - i0^+} = -i\sqrt{m|E|} = -i\sqrt{p^2} = -ip. \tag{119}$$

- For small momentum $p \ll \Lambda$,

$$\arctan \left(\frac{\Lambda}{-ip} \right) = \frac{\pi}{2} + \mathcal{O}\left(\frac{p}{\Lambda} \right), \tag{120}$$

then, Eq. (117) is given by,

$$\mathcal{A}(p) = \left[-\frac{1}{\lambda_0} - \frac{m}{4\pi^2} \left(\Lambda + ip\frac{\pi}{2} \right) \right]^{-1} = \left[-\frac{1}{\lambda_0} - \frac{m}{4\pi^2}\Lambda - ip\frac{m}{8\pi} \right]^{-1}. \tag{121}$$

- Scattering amplitude

$$f(p) = \frac{m}{8\pi}\mathcal{A}(p) = \frac{1}{-\frac{8\pi}{m}\left(\frac{1}{\lambda_0} + \frac{m}{4\pi^2}\Lambda \right) - ip}. \tag{122}$$

Comparing with Eq. (106), the scattering length is obtained as,

$$a = \frac{m}{8\pi} \left(\frac{1}{\lambda_0} + \frac{m}{4\pi^2}\Lambda \right)^{-1}. \tag{123}$$

6.5 Summary of §6

- EFT: a description of low-energy physics

- Zero-range model: nonperturbative, unitary scattering amplitude

$$f(p) = \frac{1}{-1/a - ip}. \tag{124}$$

7 Compositeness and weak-binding relation

7.1 Introduction

- Internal structure of hadron resonances: superposition of all possible configurations

$$|\Lambda(1405)\rangle = C_{3q}\,|uds\rangle + C_{5q}\,|uds\bar{q}q\rangle + C_{MB}\,|MB\rangle + \cdots. \tag{125}$$

- C_i (weights of each component) can be determined in specific models.
  → Model-dependent result (wave function is not an observable)

- A **model-independent** relation that connects observables with the internal structure?

7.2 Weak-binding relation

- **Compositeness** X of a stable bound state (deuteron) [45, 20, 21]

$$|d\rangle = \sqrt{X}\,|NN\rangle + \sqrt{Z}\,|\text{others}\rangle\,, \quad X + Z = 1. \tag{126}$$

  $|d\rangle$: wave function of the deuteron
  $|NN\rangle$: two-nucleon (s-wave) component
  (labeled by continuous variables, and X is the sum over all components)
  $|\text{others}\rangle$: all other components
  ($\sim 6q$ states, $N\Delta$ states, NN (d-wave) states, ...)
  Z: elementarity (elementariness)

- $(X, Z) \approx (1, 0)$: composite-dominant state
  $(X, Z) \approx (0, 1)$: elementary-dominant state

- **Weak-binding relation**

$$a = R\left\{\frac{2X}{1+X} + \mathcal{O}\left(\frac{R_{\text{typ}}}{R}\right)\right\}, \quad R = \frac{1}{\sqrt{2\mu B}}. \tag{127}$$

  a: NN scattering length ($^3\text{S}_1$ channel)
  B: deuteron binding energy, $\mu = M_N/2$: NN reduced mass
  R: deuteron radius (length scale associated with the binding energy)
  R_{typ}: typical interaction range

- When B is small (R_{typ}/R is negligible), the compositeness X is determined by observables.

- Conditions:

  – X is the compositeness in the s-wave scattering channel (not applicable to $\ell \neq 0$).

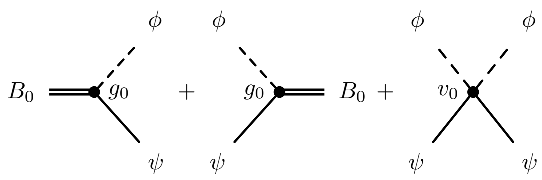

Figure 18: Feynman rules for the interaction Hamiltonian (132).

  - Stable bound state (no decay width)

- Empirical values: $B = 2.22$ MeV, $a_0 = 5.42$ fm, $R_{\rm typ} \sim 1/m_\pi = 1.43$ fm [46]

$$X = 1.68^{+3.18}_{-0.943} \quad \text{(including finite-range corrections).} \tag{128}$$

  By definition, $X \leq 1 \Rightarrow 0.74 \leq X \leq 1$: $\sim 80\%$ of the deuteron is an NN composite.

- No input on the nuclear force or wave function is required.

7.3 Compositeness in effective field theory

- Hamiltonian of EFT [34, 35]

$$H = H_{\rm free} + H_{\rm int}, \tag{129}$$

$$H_{\rm free} = \int d\boldsymbol{r} \left[\frac{1}{2M} \nabla\psi^\dagger \cdot \nabla\psi + \frac{1}{2m} \nabla\phi^\dagger \cdot \nabla\phi + \frac{1}{2M_0} \nabla B_0^\dagger \cdot \nabla B_0 + \omega_0 B_0^\dagger B_0 \right], \tag{130}$$

$$H_{\rm int} = \int d\boldsymbol{r} \left[g_0 \left(B_0^\dagger \phi\psi + \psi^\dagger\phi^\dagger B_0 \right) + v_0 \psi^\dagger\phi^\dagger\phi\psi \right], \tag{131}$$

$$\phi(\boldsymbol{r}), \psi(\boldsymbol{r}), B_0(\boldsymbol{r}) : \text{field operators}, \quad M, m, M_0 : \text{masses}, \quad \omega_0 : \text{bare energy}. \tag{132}$$

  Each term in the free Hamiltonian $H_{\rm free}$ is equivalent to the kinetic term of $\mathcal{L}_{\rm eff}$ in §6.
  g_0, v_0: coupling constants
  $H_{\rm int}$: contact interactions (Fig. 18), $\psi\phi \leftrightarrow \psi\phi$ and $\psi\phi \leftrightarrow B_0$

- Eigenstates of $H_{\rm free}$

$$H_{\rm free} |B_0\rangle = \omega_0 |B_0\rangle \quad \text{(discrete state } B_0\text{, elementary component),} \tag{133}$$

$$H_{\rm free} |\boldsymbol{p}\rangle = \frac{\boldsymbol{p}^2}{2\mu} |\boldsymbol{p}\rangle \quad (\psi\phi \text{ scattering states with } \boldsymbol{p}\text{, composite component),} \tag{134}$$

$$\langle B_0|B_0\rangle = 1, \quad \langle B_0|\boldsymbol{p}\rangle = 0, \quad \langle \boldsymbol{p}'|\boldsymbol{p}\rangle = (2\pi)^3\delta^3(\boldsymbol{p}' - \boldsymbol{p}). \tag{135}$$

- Complete set: (from particle number conservation)

$$1 = |B_0\rangle \langle B_0| + \int \frac{d\boldsymbol{p}}{(2\pi)^3} |\boldsymbol{p}\rangle \langle \boldsymbol{p}| . \tag{136}$$

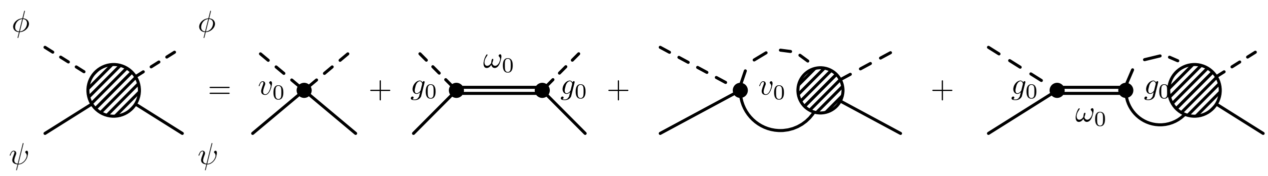

Figure 19: Feynman diagrams of the $\psi\phi$ scattering amplitude.

Relation to Feshbach projection [47] ($\hat{P} + \hat{Q} = \hat{I}$)

$$\hat{P} = \int \frac{d\boldsymbol{p}}{(2\pi)^3} |\boldsymbol{p}\rangle \langle\boldsymbol{p}| \quad \text{(projection onto } \psi\phi \text{ scattering states)}, \tag{137}$$

$$\hat{Q} = |B_0\rangle \langle B_0| \quad \text{(projection onto discrete state } B_0). \tag{138}$$

Field theory equivalent to the single-resonance approximation of Q channel in §5

- Bound state $|B\rangle$ with binding energy B as an eigenstate of H (physical state)

$$H |B\rangle = -B |B\rangle . \tag{139}$$

Compositeness X, elementarity Z

$$X \equiv \langle B| \hat{P} |B\rangle = \int \frac{d\boldsymbol{p}}{(2\pi)^3} |\langle \boldsymbol{p}|B\rangle|^2 \geq 0 \quad \text{(overlap with scattering states)}, \tag{140}$$

$$Z \equiv \langle B| \hat{Q} |B\rangle = |\langle B_0|B\rangle|^2 \geq 0 \quad \text{(overlap with discrete state)}. \tag{141}$$

- From the normalization $\langle B|B\rangle = 1$ and the completeness relation (136),

$$Z + X = 1. \tag{142}$$

X and Z can be interpreted as **probabilities** ← (140), (141), and (142)

7.4 Weak-binding relation in effective field theory

- $\psi\phi$ scattering amplitude (derived as in §6, see Fig. 19)

$$f(E) = -\frac{\mu}{2\pi} \frac{1}{1/v(E) - G(E)}, \tag{143}$$

$$v(E) = v_0 + \frac{g_0^2}{E - \omega_0}, \tag{144}$$

$$G(E) = \frac{1}{2\pi^2} \int_0^\Lambda dq \frac{q^2}{E - q^2/(2\mu) + i0^+}. \tag{145}$$

- Cutoff Λ: momentum scale at which the hadron interaction can be regarded as pointlike

$$\Rightarrow R_{\text{typ}} = \frac{1}{\Lambda}. \tag{146}$$

- Expression for the compositeness in terms of the scattering amplitude

$$X = \left. \frac{G'(E)}{G'(E) - [1/v(E)]'} \right|_{E=-B}, \quad A'(E) = \frac{dA(E)}{dE}. \tag{147}$$

- Expansion of the scattering length in powers of (R_{typ}/R)

$$\begin{aligned} a &= -f(E=0) = \frac{\mu}{2\pi}\left[1/v(0) - G(0)\right]^{-1} \\ &= \cdots = R\left\{\frac{2X}{1+X} + \mathcal{O}\left(\frac{R_{\text{typ}}}{R}\right)\right\}, \quad R = \frac{1}{\sqrt{2\mu B}}. \end{aligned} \tag{148}$$

- If $\mathcal{O}(R_{\text{typ}}/R)$ is negligible, **compositeness** $X \leftarrow (a, B)$

7.5 Generalization to unstable states

- For applications to hadron resonances, a generalization to unstable states is necessary.
- Inclusion of a decay channel (Fig. 20)
  Fields: ϕ_1, ψ_1, ϕ_2, ψ_2, B_0
  Four-point contact interactions: $\psi_1\phi_1 \leftrightarrow \psi_1\phi_1$, $\psi_1\phi_1 \leftrightarrow \psi_2\phi_2$, $\psi_2\phi_2 \leftrightarrow \psi_2\phi_2$
  Three-point contact interactions: $\psi_1\phi_1 \leftrightarrow B_0$, $\psi_2\phi_2 \leftrightarrow B_0$
- When the threshold energy $-\nu$ of the additional channel 2 ($\psi_2\phi_2$) is lower than B (§5),

$$H|R\rangle = E_h|R\rangle, \quad E_h \in \mathbb{C}. \tag{149}$$

- Normalization condition for resonances ($\langle R|R\rangle$ diverges)

$$\langle \tilde{R}|R\rangle = 1. \tag{150}$$

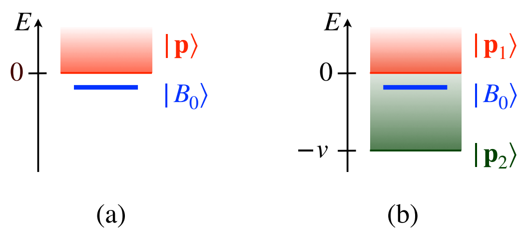

Figure 20: Spectrum of free Hamiltonian. (a): EFT in Sec. 7.3 and 7.4, (b): EFT in Sec. 7.5.

$\langle\tilde{R}|$ is the left eigenvector with the same complex eigenvalue,

$$\langle\tilde{R}|\, H = E_h \,\langle\tilde{R}|\,. \tag{151}$$

(Because of the non-hermiticity, left eigenvector is not conjugate of right eigenvector)

- Complete set

$$1 = \hat{P} + \hat{Q}, \tag{152}$$
$$\hat{P} = \int \frac{d\boldsymbol{p}}{(2\pi)^3} \,|\boldsymbol{p}_1\rangle \langle\boldsymbol{p}_1| \quad \text{(projection onto } \psi_1\phi_1 \text{ scattering states)}, \tag{153}$$
$$\hat{Q} = |B_0\rangle \langle B_0| + \int \frac{d\boldsymbol{p}}{(2\pi)^3} \,|\boldsymbol{p}_2\rangle \langle\boldsymbol{p}_2| \quad \text{(projection onto } B_0 \text{ and } \psi_2\phi_2). \tag{154}$$

- Compositeness X, elementarity Z:

$$X = \langle\tilde{R}|\, P\, |R\rangle = \int \frac{d\boldsymbol{p}}{(2\pi)^3} \langle\tilde{R}|\boldsymbol{p}_1\rangle \langle\boldsymbol{p}_1|R\rangle \in \mathbb{C}, \tag{155}$$
$$Z = \langle\tilde{R}|\, Q\, |R\rangle = \langle\tilde{R}|B_0\rangle \langle B_0|R\rangle + \int \frac{d\boldsymbol{p}}{(2\pi)^3} \langle\tilde{R}|\boldsymbol{p}_2\rangle \langle\boldsymbol{p}_2|R\rangle \in \mathbb{C}. \tag{156}$$

- While $X+Z = 1$ still holds, each term is **complex** and cannot be interpreted as a probability.
- Expand the scattering length of channel 1 by $(R_{\rm typ}/R)$ (R and a are complex)

$$a = R\left\{\frac{2X}{1+X} + \mathcal{O}\left(\left|\frac{R_{\rm typ}}{R}\right|\right) + \mathcal{O}\left(\left|\frac{l}{R}\right|^3\right)\right\}, \quad R = \frac{1}{\sqrt{-2\mu E_h}}, \quad l = \frac{1}{\sqrt{2\mu\nu}}. \tag{157}$$

ν: threshold energy difference, l: corresponding length scale

- If $\mathcal{O}(R_{\rm typ}/R)$ and $\mathcal{O}(|l/R|^3)$ are negligible, **compositeness** $X \leftarrow (a, E_h)$
- Several interpretation of complex X [34, 35, 48, 49, 50, 30], but no consensus is reached.
- $\Lambda(1405)$ case:
  - Channel 1 is $\bar{K}N$, channel 2 is $\pi\Sigma$
  - Inputs: $E_h = -10 - 26i$ MeV, $a = 1.39 - 0.85i$ fm [51, 52]
  - For $|R| \sim 2$ fm, $R_{\rm typ} \sim 0.25$ fm (ρ-meson exchange), $l \sim 1.08$ fm ($\pi\Sigma$ channel)

Neglecting the correction terms, we obtain,

$$X = 1.2 + i0.1. \tag{158}$$

X is close to 1 $\Rightarrow$ **the $\bar{K}N$ molecular component is dominant**.

8 Spin-1/2 states

8.1 State representation

- Pauli spinor (quantum bit, **qubit**): two-component complex vector

$$|\psi\rangle = \begin{pmatrix} \alpha \\ \beta \end{pmatrix}, \quad \alpha, \beta \in \mathbb{C}, \tag{159}$$

$$\langle\psi| = |\psi\rangle^\dagger = \begin{pmatrix} \alpha^* & \beta^* \end{pmatrix}. \tag{160}$$

Four degrees of freedom (Re α, Im α, Re β, Im β without any constraint, $|\psi\rangle \in \mathcal{H} = \mathbb{C}^2$)

- Normalization and phase of the wave function

$$\langle\psi|\psi\rangle = 1 \quad \Rightarrow \quad |\alpha|^2 + |\beta|^2 = 1. \tag{161}$$

(In the following, all state vectors are assumed to be normalized)
Phase transformation $|\psi\rangle \to e^{i\eta}|\psi\rangle$ ($\eta \in \mathbb{R}$) does not change expectation values.
$\to$ $|\psi\rangle$ is described by **two degrees of freedom**.

- Bloch-sphere representation

$$|\theta, \phi\rangle = \begin{pmatrix} \cos\frac{\theta}{2} \\ \sin\frac{\theta}{2} e^{i\phi} \end{pmatrix}, \quad 0 \le \theta < \pi, \quad 0 \le \phi < 2\pi. \tag{162}$$

Two real parameters $\theta, \phi \in \mathbb{R}$: angular part of three-dimensional polar coordinates

- Fubini–Study measure (generalizable to higher-spin states)
Normalization and phase: equivalence class by complex scalar multiplication

$$|\psi\rangle \sim \lambda\,|\psi\rangle, \quad \lambda \in \mathbb{C}^\times. \tag{163}$$

Quotient space $\mathbb{C}^2/\sim \,\simeq\, \mathbb{CP}^1$ (complex projective space)

$$|\theta_1, \nu_1\rangle = \begin{pmatrix} \cos\theta_1 \\ \sin\theta_1 e^{i\nu_1} \end{pmatrix}, \quad 0 \le \theta_1 < \frac{\pi}{2}, \quad 0 \le \nu_1 < 2\pi. \tag{164}$$

Two degrees of freedom θ_1, ν_1

- Spin operator $\boldsymbol{s}$: represented by Pauli matrices $\boldsymbol{\sigma}$

$$\boldsymbol{s} = \frac{\boldsymbol{\sigma}}{2}, \quad \sigma_x = \begin{pmatrix} 0 & 1 \\ 1 & 0 \end{pmatrix}, \quad \sigma_y = \begin{pmatrix} 0 & -i \\ i & 0 \end{pmatrix}, \quad \sigma_z = \begin{pmatrix} 1 & 0 \\ 0 & -1 \end{pmatrix}. \tag{165}$$

(In quantum information science, $\sigma_x = X$, $\sigma_y = Y$, $\sigma_z = Z$)

- Eigenstates of s_z

$$|\uparrow\rangle = \begin{pmatrix} 1 \\ 0 \end{pmatrix}, \quad |\downarrow\rangle = \begin{pmatrix} 0 \\ 1 \end{pmatrix}, \tag{166}$$

$$s_z |\uparrow\rangle t = \frac{1}{2} |\uparrow\rangle, \quad s_z |\downarrow\rangle = -\frac{1}{2} |\downarrow\rangle. \tag{167}$$

(In quantum information science, $|\uparrow\rangle = |0\rangle$, $|\downarrow\rangle = |1\rangle$)

- Eigenstates of s_x and s_y

$$|+\rangle = \frac{1}{\sqrt{2}} \begin{pmatrix} 1 \\ 1 \end{pmatrix}, \quad |-\rangle = \frac{1}{\sqrt{2}} \begin{pmatrix} 1 \\ -1 \end{pmatrix}, \tag{168}$$

$$s_x |+\rangle = \frac{1}{2} |+\rangle, \quad s_x |-\rangle = -\frac{1}{2} |-\rangle, \tag{169}$$

$$|+i\rangle = \frac{1}{\sqrt{2}} \begin{pmatrix} 1 \\ i \end{pmatrix}, \quad |-i\rangle = \frac{1}{\sqrt{2}} \begin{pmatrix} 1 \\ -i \end{pmatrix}, \tag{170}$$

$$s_y |+i\rangle = \frac{1}{2} |+i\rangle, \quad s_y |-i\rangle = -\frac{1}{2} |-i\rangle. \tag{171}$$

8.2 State transformations (quantum gates)

- **Unitary operator** U

$$U^\dagger U = UU^\dagger = 1, \quad U^\dagger = U^{-1}. \tag{172}$$

All Pauli matrices are Hermitian and unitary

- U transforms a state into another state: a **quantum gate** acting on a qubit

$$|\phi\rangle = U |\psi\rangle. \tag{173}$$

- Norm (probability) is preserved under a unitary transformation.

$$\langle\phi|\phi\rangle = \langle\psi| U^\dagger U |\psi\rangle = \langle\psi|\psi\rangle. \tag{174}$$

The time evolution of a system is described by a unitary operator

- Example: X gate

$$\sigma_x |\uparrow\rangle = |\downarrow\rangle, \quad \sigma_x |\downarrow\rangle = |\uparrow\rangle. \tag{175}$$

Exchanges spin-up and spin-down (swaps 0 and 1: classical NOT gate)

- Hadamard gate,

$$H = \frac{\sigma_x + \sigma_z}{\sqrt{2}} = \frac{1}{\sqrt{2}}\begin{pmatrix} 1 & 1 \\ 1 & -1 \end{pmatrix}, \tag{176}$$

maps the z basis to the x basis (A 180° rotation about the axis $(1,0,1)/\sqrt{2}$)

$$H\left|\uparrow\right\rangle = \left|+\right\rangle, \quad H\left|\downarrow\right\rangle = \left|-\right\rangle, \tag{177}$$

$$H\left|+\right\rangle = \left|\uparrow\right\rangle, \quad H\left|-\right\rangle = \left|\downarrow\right\rangle. \tag{178}$$

- Time reversal (not unitary operator)

$$T = -i\sigma_y K, \quad T\begin{pmatrix} \alpha \\ \beta \end{pmatrix} = \begin{pmatrix} -\beta^* \\ \alpha^* \end{pmatrix}. \tag{179}$$

K: complex cojugate
Under T, $\boldsymbol{r} \to \boldsymbol{r}$, $\boldsymbol{p} \to -\boldsymbol{p}$, $\boldsymbol{\ell} \to -\boldsymbol{\ell}$: T corresponds to **spin flip**

$$T\left|\uparrow\right\rangle \propto \left|\downarrow\right\rangle, \quad T\left|+\right\rangle \propto \left|-\right\rangle, \quad \cdots, \quad T\left|\theta, \phi\right\rangle \propto \left|\pi - \theta, \phi + \pi\right\rangle \tag{180}$$

8.3 Projective measurement

- Finite-dimensional Hilbert space without degeneracy
- Physical observables are represented by **Hermitian operators**.
- A Hermitian operator O can be diagonalized by a unitary operator U,

$$U^{-1}OU = \begin{pmatrix} \lambda_1 & 0 & \cdots \\ 0 & \lambda_2 & \cdots \\ \vdots & \vdots & \ddots \end{pmatrix}, \quad \lambda_i \in \mathbb{R}. \tag{181}$$

- **Spectral decomposition**: representation of O in terms of its eigenbasis $\{\left|i\right\rangle\}$

$$O = \sum_i \lambda_i \left|i\right\rangle \left\langle i\right|. \tag{182}$$

- Complete orthonormal system (**CONS**) $\{\left|i\right\rangle\}$

$$\left\langle i|j\right\rangle = \delta_{ij}, \quad \sum_i \left|i\right\rangle\left\langle i\right| = 1. \tag{183}$$

The eigenvectors of a Hermitian operator can always be chosen to form a CONS.
Example: $\{\left|\uparrow\right\rangle, \left|\downarrow\right\rangle\}$ (computational basis)

- **Projection operator** onto the eigenstate with eigenvalue λ_i

$$P_i = |i\rangle \langle i| \,. \tag{184}$$

Orthonomality

$$P_i P_j = \delta_{ij} P_i, \quad \sum_i P_i = 1. \tag{185}$$

- Expansion of a state $|\psi\rangle$ in the basis $\{|i\rangle\}$

$$|\psi\rangle = \sum_i |i\rangle \langle i|\psi\rangle = \sum_i C_i |i\rangle \,, \quad C_i = \langle i|\psi\rangle \,. \tag{186}$$

Example:

$$|+\rangle = \frac{1}{\sqrt{2}} |\uparrow\rangle + \frac{1}{\sqrt{2}} |\downarrow\rangle \,, \quad \langle \uparrow |+\rangle = \frac{1}{\sqrt{2}}, \quad \langle \downarrow |+\rangle = \frac{1}{\sqrt{2}}, \tag{187}$$

$$|\psi\rangle = \begin{pmatrix} \alpha \\ \beta \end{pmatrix} = \alpha |\uparrow\rangle + \beta |\downarrow\rangle \,, \quad \langle \uparrow |\psi\rangle = \alpha, \quad \langle \downarrow |\psi\rangle = \beta. \tag{188}$$

- **Born rule**: measurement of $O \to$ one of $\{\lambda_i\}$ is obtained with **probability**,

$$\mathrm{Pr}(i) = |C_i|^2 = |\, \langle i|\psi\rangle \,|^2, \tag{189}$$

and the state collapses to $|i\rangle$,

$$|\psi\rangle \to |i\rangle = \frac{P_i |\psi\rangle}{\| P_i |\psi\rangle \|}. \tag{190}$$

- Example: $O = s_z$, with CONS $\{|\uparrow\rangle, |\downarrow\rangle\}$

$$P_\uparrow = |\uparrow\rangle \langle \uparrow| = \begin{pmatrix} 1 & 0 \\ 0 & 0 \end{pmatrix}, \quad P_\downarrow = |\downarrow\rangle \langle \downarrow| = \begin{pmatrix} 0 & 0 \\ 0 & 1 \end{pmatrix}, \tag{191}$$

$$\mathrm{Pr}(\uparrow) = |\, \langle \uparrow |\psi\rangle \,|^2. \tag{192}$$

- **Expectation value** of O

$$\langle \psi| O |\psi\rangle = \langle \psi| \left(\sum_i \lambda_i |i\rangle \langle i| \right) |\psi\rangle = \sum_i \mathrm{Pr}(i) \lambda_i. \tag{193}$$

Sum of (probability)×(outcome)

8.4 Density matrix

- **Density matrix** (density operator) ρ corresponding to a normalized state $|\psi\rangle$

$$\rho = |\psi\rangle \langle\psi| \,. \tag{194}$$

  Hermiticity: $\rho^\dagger = \rho \to$ nonnegative eigenvalues

- **Trace** of an operator O: sum of diagonal matrix elements in any CONS $\{|i\rangle\}$

$$\mathrm{Tr}\,[O] = \sum_i \langle i|O|i\rangle = \sum_i \lambda_i. \tag{195}$$

  Result is independent of the choice of CONS.

- Normalization of the state

$$\mathrm{Tr}\,[\rho] = \sum_i \langle i|\psi\rangle \langle\psi|i\rangle = \langle\psi|\psi\rangle = 1. \tag{196}$$

- Probability (by density matrix)

$$\mathrm{Pr}(i) = \mathrm{Tr}\,[P_i\rho] \,. \tag{197}$$

- Expectation value (by density matrix)

$$\langle\psi| \, O \, |\psi\rangle = \mathrm{Tr}\,[O\rho] \,. \tag{198}$$

- Example: expectation values of Pauli matrices for the Bloch-sphere state $\rho = |\theta,\phi\rangle \langle\theta,\phi|$

$$\mathrm{Tr}\,[\sigma_x\rho] = \sin\theta\cos\phi \tag{199}$$

$$\mathrm{Tr}\,[\sigma_y\rho] = \sin\theta\sin\phi \tag{200}$$

$$\mathrm{Tr}\,[\sigma_z\rho] = \cos\theta. \tag{201}$$

  These correspond to the Cartesian coordinates of a point on the unit sphere.

9 Two-spin system and entanglement entropy

9.1 Representation of two-spin states

- Composite system of spin A and spin B: $\mathcal{H} = \mathcal{H}_A \otimes \mathcal{H}_B$
(in quantum information science, a two-qubit system of Alice and Bob)

- **Tensor-product states**

$$|\uparrow\uparrow\rangle = |\uparrow_A\rangle \otimes |\uparrow_B\rangle\,, \quad |\uparrow\downarrow\rangle\,, \quad |\downarrow\uparrow\rangle\,, \quad |\downarrow\downarrow\rangle\,. \tag{202}$$

- Spin operators for each subsystem

$$\boldsymbol{s}_A = \underbrace{\boldsymbol{s}}_{\text{acts on } A} \otimes \underbrace{1}_{\text{acts on } B}\,, \quad \boldsymbol{s}_B = 1 \otimes \boldsymbol{s}. \tag{203}$$

- Action of operators

$$(s_A)_z\,|\uparrow\uparrow\rangle = \frac{1}{2}\,|\uparrow\uparrow\rangle\,, \quad \ldots \tag{204}$$

- Total spin operator $\boldsymbol{S}$

$$\boldsymbol{S} = \boldsymbol{s}_A + \boldsymbol{s}_B. \tag{205}$$

- Eigenstates of $\boldsymbol{S}$: labeled by total spin $S = 0, 1$ and z-component S_z

$$|S, S_z\rangle = \underbrace{|0,0\rangle}_{S=0}, \quad \underbrace{|1,1\rangle\,, \quad |1,0\rangle\,, \quad |1,-1\rangle}_{S=1}. \tag{206}$$

Action of spin operators

$$S_z\,|1,-1\rangle = -\,|1,-1\rangle\,, \quad \boldsymbol{S}^2\,|1,-1\rangle = S(S+1)\,|1,-1\rangle = 2\,|1,-1\rangle\,, \quad \ldots \tag{207}$$

- Kronecker product of states: representation as 4-component vectors

$$|\uparrow\uparrow\rangle = \begin{pmatrix} 1 \\ 0 \end{pmatrix} \otimes \begin{pmatrix} 1 \\ 0 \end{pmatrix} = \begin{pmatrix} 1 \times \begin{pmatrix} 1 \\ 0 \end{pmatrix} \\ 0 \times \begin{pmatrix} 1 \\ 0 \end{pmatrix} \end{pmatrix} = \begin{pmatrix} 1 \\ 0 \\ 0 \\ 0 \end{pmatrix}, \tag{208}$$

$$|\uparrow\downarrow\rangle = \begin{pmatrix} 0 \\ 1 \\ 0 \\ 0 \end{pmatrix}, \quad |\downarrow\uparrow\rangle = \begin{pmatrix} 0 \\ 0 \\ 1 \\ 0 \end{pmatrix}, \quad |\downarrow\downarrow\rangle = \begin{pmatrix} 0 \\ 0 \\ 0 \\ 1 \end{pmatrix}. \tag{209}$$

- Kronecker product of operators: 4×4 matrices

$$(s_A)_x = s_x \otimes 1 = \frac{1}{2}\begin{pmatrix} 0 & 1 \\ 1 & 0 \end{pmatrix} \otimes \begin{pmatrix} 1 & 0 \\ 0 & 1 \end{pmatrix}$$
$$= \frac{1}{2}\begin{pmatrix} 0 \times \begin{pmatrix} 1 & 0 \\ 0 & 1 \end{pmatrix} & 1 \times \begin{pmatrix} 1 & 0 \\ 0 & 1 \end{pmatrix} \\ 1 \times \begin{pmatrix} 1 & 0 \\ 0 & 1 \end{pmatrix} & 0 \times \begin{pmatrix} 1 & 0 \\ 0 & 1 \end{pmatrix} \end{pmatrix} = \frac{1}{2}\begin{pmatrix} 0 & 0 & 1 & 0 \\ 0 & 0 & 0 & 1 \\ 1 & 0 & 0 & 0 \\ 0 & 1 & 0 & 0 \end{pmatrix}, \tag{210}$$

$$s_x \otimes s_x = \frac{1}{2}\begin{pmatrix} 0 & 1 \\ 1 & 0 \end{pmatrix} \otimes \frac{1}{2}\begin{pmatrix} 0 & 1 \\ 1 & 0 \end{pmatrix}$$
$$= \frac{1}{4}\begin{pmatrix} 0 \times \begin{pmatrix} 0 & 1 \\ 1 & 0 \end{pmatrix} & 1 \times \begin{pmatrix} 0 & 1 \\ 1 & 0 \end{pmatrix} \\ 1 \times \begin{pmatrix} 0 & 1 \\ 1 & 0 \end{pmatrix} & 0 \times \begin{pmatrix} 0 & 1 \\ 1 & 0 \end{pmatrix} \end{pmatrix} = \frac{1}{4}\begin{pmatrix} 0 & 0 & 0 & 1 \\ 0 & 0 & 1 & 0 \\ 0 & 1 & 0 & 0 \\ 1 & 0 & 0 & 0 \end{pmatrix}. \tag{211}$$

- Density matrix of a tensor-product state: $\rho = \rho_a \otimes \rho_b$ holds

$$\begin{pmatrix} 1 & 0 & 0 & 0 \\ 0 & 0 & 0 & 0 \\ 0 & 0 & 0 & 0 \\ 0 & 0 & 0 & 0 \end{pmatrix} = |\uparrow\uparrow\rangle\langle\uparrow\uparrow| = \underbrace{|\uparrow\rangle\langle\uparrow|}_{\rho_a} \otimes \underbrace{|\uparrow\rangle\langle\uparrow|}_{\rho_b} = \begin{pmatrix} 1 & 0 \\ 0 & 0 \end{pmatrix} \otimes \begin{pmatrix} 1 & 0 \\ 0 & 0 \end{pmatrix}. \tag{212}$$

9.2 Complete orthonormal systems

- **Computational basis**: $\{|\uparrow\uparrow\rangle, |\uparrow\downarrow\rangle, |\downarrow\uparrow\rangle, |\downarrow\downarrow\rangle\}$
- **Bell basis**: $\{|\Phi^+\rangle, |\Phi^-\rangle, |\Psi^+\rangle, |\Psi^-\rangle\}$

$$|\Phi^\pm\rangle = \frac{|\uparrow\uparrow\rangle \pm |\downarrow\downarrow\rangle}{\sqrt{2}} \quad \text{(not eigenstates of the total spin } \boldsymbol{S}\text{)}, \tag{213}$$
$$|\Psi^\pm\rangle = \frac{|\uparrow\downarrow\rangle \pm |\downarrow\uparrow\rangle}{\sqrt{2}} \quad \text{(states with } S_z = 0\text{, corresponding to } S = 1 \text{ and } S = 0\text{)}. \tag{214}$$

- General two-spin state (vector in $\mathbb{C}^4$)

$$|\Psi\rangle = \alpha|\uparrow\uparrow\rangle + \beta|\uparrow\downarrow\rangle + \gamma|\downarrow\uparrow\rangle + \delta|\downarrow\downarrow\rangle = \begin{pmatrix} \alpha \\ \beta \\ \gamma \\ \delta \end{pmatrix}, \quad \alpha, \beta, \gamma, \delta \in \mathbb{C}. \tag{215}$$

Normalization

$$|\alpha|^2 + |\beta|^2 + |\gamma|^2 + |\delta|^2 = 1. \tag{216}$$

- General state $|\Psi\rangle$: using CONS $\{|i_A\rangle\}$ of $\mathcal{H}_A$ and $\{|j_B\rangle\}$ of $\mathcal{H}_B$

$$|\Psi\rangle = \sum_{i,j} \alpha_{ij} |i_A\rangle \otimes |j_B\rangle, \quad \alpha_{ij} \in \mathbb{C} \quad \text{(sum over } i \text{ and } j\text{)}. \tag{217}$$

- **Schmidt decomposition**: there exist CONS $\{|i'_A\rangle\}$ and $\{|i'_B\rangle\}$ such that[5]

$$|\Psi\rangle = \sum_{i=1}^{l} \sqrt{p_i}\, |i'_A\rangle \otimes |i'_B\rangle \quad \text{(sum over a common } i\text{)}, \quad \sum_{i=1}^{l} p_i = 1. \tag{218}$$

  $p_i > 0$: Schmidt coefficients, l: Schmidt rank
  Shown by the singular value decomposition of α_{ij} (also valid for $\dim \mathcal{H}_A \neq \dim \mathcal{H}_B$)

9.3 Entropy of quantum systems

- **von Neumann entropy** by the density matrix ρ

$$S(\rho) = -\mathrm{Tr}\left[\rho \log \rho\right]. \tag{219}$$

  Expanding $\rho = \sum_i \lambda_i |i\rangle \langle i|$ in its eigenbasis $\{|i\rangle\}$,

$$S(\rho) = -\sum_i \lambda_i \log \lambda_i. \tag{220}$$

  Shannon entropy of the eigenvalue distribution λ_i

- Example: canonical ensemble $\rho = e^{-\beta H}/Z$

$$\begin{aligned} S(\rho) &= -\mathrm{Tr}\left[\rho \log(e^{-\beta H}/Z)\right] \\ &= -\mathrm{Tr}\left[\rho(-\beta H - \log Z)\right] \\ &= \beta \mathrm{Tr}\left[\rho H\right] + \log Z \ \mathrm{Tr}\left[\rho\right] \\ &= \beta E + \log Z \\ &= \beta E - \beta F, \\ F &= E - TS. \end{aligned} \tag{221}$$

- **Entanglement (von Neumann) entropy**: quantifies correlations between A and B (see Sec. 10 for details)

$$\mathcal{E}_{\mathrm{vN}} = -\mathrm{Tr}_A\left[\rho_A \log \rho_A\right]. \tag{222}$$

  Information lost by tracing out the system B

[5] Strictly speaking, these form an orthonormal set (ONS) in the full space; zero singular values are omitted.

- **Reduced density matrix**: for the general state in Eq. (215),

$$\rho_A = \mathrm{Tr}_B\left[\rho\right] = \begin{pmatrix} |\alpha|^2 + |\beta|^2 & \alpha\gamma^* + \beta\delta^* \\ \alpha^*\gamma + \beta^*\delta & |\gamma|^2 + |\delta|^2 \end{pmatrix}. \tag{223}$$

Partial trace over spin B: gives the density matrix in $\mathcal{H}_A$

$$\mathrm{Tr}_B\left[\rho\right] = \sum_i (1 \otimes \langle i_B|)\ \rho\ (1 \otimes |i_B\rangle). \tag{224}$$

If $\rho = \rho_a \otimes \rho_b$ (product state),

$$\mathrm{Tr}_B\left[\rho_a \otimes \rho_b\right] = \rho_a \mathrm{Tr}_B\left[\rho_b\right]. \tag{225}$$

- Using the Schmidt decomposition,

$$\rho = |\Psi\rangle\langle\Psi| = \sum_{i,j} \sqrt{p_i p_j}\, |i_A\rangle\langle j_A| \otimes |i_B\rangle\langle j_B|, \tag{226}$$

$$\begin{aligned} \mathrm{Tr}_B\left[\rho\right] &= \sum_{i,j,k} \sqrt{p_i p_j}\, |i_A\rangle\langle j_A| \otimes \langle k_B|i_B\rangle\langle j_B|k_B\rangle = \sum_{i,j} \sqrt{p_i p_j}\, |i_A\rangle\langle j_A|\, \delta_{ij} \\ &= \sum_i p_i\, |i_A\rangle\langle i_A|. \end{aligned} \tag{227}$$

Since $\mathrm{Tr}_A\left[\rho\right]$ has the same eigenvalues p_i,

$$\mathcal{E}_{\mathrm{vN}} = -\mathrm{Tr}_A\left[\rho_A \log \rho_A\right] = -\mathrm{Tr}_B\left[\rho_B \log \rho_B\right]. \tag{228}$$

9.4 Measures of quantum correlations

- **Linear entropy** ($\log \rho_A = \log[1 + (\rho_A - 1)] = \rho_A - 1 + \cdots$)

$$\mathcal{E} = 1 - \mathrm{Tr}_A\left[\rho_A^2\right]. \tag{229}$$

- Concurrence [53, 54]

$$\Delta = |\langle\Psi|\sigma_y \otimes \sigma_y|\Psi^*\rangle| = 2|\alpha\delta - \beta\gamma|. \tag{230}$$

From Eq. (179), Δ is the inner product with the spin-flipped state.

- Any entanglement measure defined from ρ_A (by density matrix) can be expressed in terms of Δ,

$$\mathcal{E}_{\mathrm{vN}} = -\lambda_+ \log \lambda_+ - \lambda_- \log \lambda_-, \quad \lambda_\pm = \frac{1}{2}(1 \pm \sqrt{1 - \Delta^2}), \tag{231}$$

$$\mathcal{E} = \frac{1}{2}\Delta^2 = 2|\alpha\delta - \beta\gamma|^2. \tag{232}$$

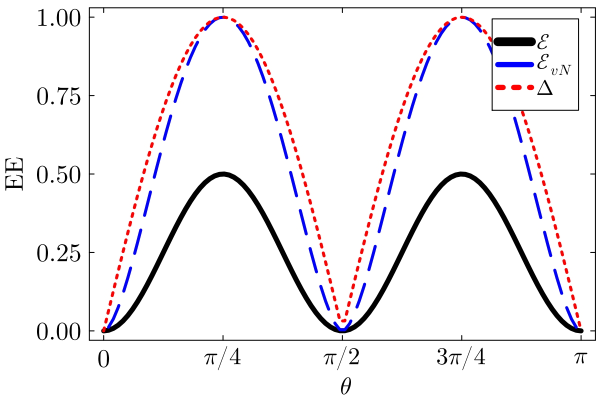

θ	0	$\pi/4$	$\pi/2$	$3\pi/4$
$\vert\psi\rangle$	$\vert\uparrow\downarrow\rangle$	$\vert\Psi^+\rangle$	$\vert\downarrow\uparrow\rangle$	$-\vert\Psi^-\rangle$
$\mathcal{E}$	0	$1/2$	0	$1/2$
$\mathcal{E}_{\rm vN}$	0	1	0	1
Δ	0	1	0	1

Figure 21: Linear entropy $\mathcal{E}$, von Neumann entropy $\mathcal{E}_{\rm vN}$, and concurrence Δ for the state (241).

- Entanglement of a **product state** $|\uparrow\downarrow\rangle$

$$\beta = 1, \quad \alpha = \gamma = \delta = 0, \tag{233}$$

$$\Delta = 0, \tag{234}$$

$$\mathcal{E} = 0, \tag{235}$$

$$\lambda_+ = 1, \quad \lambda_- = 0 \quad \Rightarrow \quad \mathcal{E}_{\rm vN} = 0. \tag{236}$$

All measures vanish: 0

- Entanglement of a **Bell state** $|\Psi^+\rangle$

$$\alpha = \delta = 0, \quad \beta = \gamma = \frac{1}{\sqrt{2}}, \tag{237}$$

$$\Delta = 1, \tag{238}$$

$$\mathcal{E} = \frac{1}{2}, \tag{239}$$

$$\lambda_+ = \frac{1}{2}, \quad \lambda_- = \frac{1}{2} \quad \Rightarrow \quad \mathcal{E}_{\rm vN} = \log 2 = 1. \tag{240}$$

1 ebit (entanglement bit), the fundamental unit of entanglement[6]

- General superposition state

$$|\psi\rangle = \cos\theta\,|\uparrow\downarrow\rangle + \sin\theta\,|\downarrow\uparrow\rangle\,. \tag{241}$$

Fig. 21: comparison of $\mathcal{E}$, $\mathcal{E}_{\rm vN}$, and Δ

$\mathcal{E}_{\rm vN} = \mathcal{E} = \Delta_{\rm vN} = 0$ for product states ($\theta = 0, \pi/2$), while they become **maximal** for Bell states ($\theta = \pi/4, 3\pi/4$).

[6] In quantum information, the logarithm is taken with base 2.

10 Classical and quantum correlations

10.1 Pure and mixed states

- **Pure state**: density matrix by a single state

$$\rho = |\psi\rangle \langle\psi| . \tag{242}$$

Property (idempotency): ρ is a projection operator

$$\rho^2 = |\psi\rangle \underbrace{\langle\psi|\psi\rangle}_{=1} \langle\psi| = |\psi\rangle \langle\psi| = \rho, \tag{243}$$

$$\mathrm{Tr}\left[\rho^2\right] = \mathrm{Tr}\left[\rho\right] = 1 \quad \text{(pure state)}. \tag{244}$$

- **Mixed state**: density matrix by a weighted sum of states with **real** coefficients $0 \leq p_i \leq 1$

$$\rho = \sum_i p_i |i\rangle \langle i| , \quad \sum_i p_i = 1. \tag{245}$$

An ensemble of states prepared with probability p_i ("mixed ensemble" in J.J. Sakurai)
Classical probabilistic mixture of states, **not** a quantum superposition
The decomposition of a mixed state is not unique (Schrödinger's mixture theorem).

- A mixed state is normalized but does not satisfy $\rho^2 = \rho$:

$$\mathrm{Tr}\left[\rho\right] = \sum_i p_i \mathrm{Tr}\left[|i\rangle \langle i|\right] = \sum_i p_i = 1, \tag{246}$$

$$\rho^2 = \sum_{i,j} p_i p_j |i\rangle \langle i|j\rangle \langle j| = \sum_i p_i^2 |i\rangle \langle i| \neq \rho. \tag{247}$$

For $0 \leq p_i \leq 1$, $\sum_i p_i^2 \leq \sum_i p_i$, therefore

$$\mathrm{Tr}\left[\rho^2\right] \leq 1 \quad \text{(mixed state)}. \tag{248}$$

Equality holds for a pure state.

- **Purity** $\mathrm{Tr}\left[\rho^2\right]$: distance from a pure state

$$\underbrace{1}_{\text{pure state}} \geq \mathrm{Tr}\left[\rho^2\right] \geq \underbrace{\frac{1}{d}}_{\text{maximally mixed state}}, \quad d = \dim \mathcal{H}. \tag{249}$$

Equalities hold for

$$\{p_i\} = \begin{cases} \{1, 0, \ldots, 0\} & \text{(pure state, rank}(\rho) = 1) \\ \{1/d, 1/d, \ldots, 1/d\} & \text{(maximally mixed state, } \rho \propto 1) \end{cases}. \tag{250}$$

- Example: pure states for a single-spin system

$$|\uparrow\rangle\langle\uparrow| = \begin{pmatrix} 1 & 0 \\ 0 & 0 \end{pmatrix}, \tag{251}$$

$$|+\rangle\langle+| = \begin{pmatrix} 1/2 & 1/2 \\ 1/2 & 1/2 \end{pmatrix}, \quad |+\rangle = \frac{1}{\sqrt{2}}|\uparrow\rangle + \frac{1}{\sqrt{2}}|\downarrow\rangle. \tag{252}$$

After diagonalization, Eq. (252) takes the same form as Eq. (251).

- Example: mixed state for a single-spin system

$$\frac{1}{2}|\uparrow\rangle\langle\uparrow| + \frac{1}{2}|\downarrow\rangle\langle\downarrow| = \begin{pmatrix} 1/2 & 0 \\ 0 & 1/2 \end{pmatrix} = \frac{1}{2}|+\rangle\langle+| + \frac{1}{2}|-\rangle\langle-|. \tag{253}$$

Formally, this is $|+\rangle\langle+|$ without the off-diagonal elements.

10.2 Correlations between two spins

- **Measurement** of s_z of both spins A and B for a two-spin state $|\psi\rangle$
  The probability of obtaining both spins up is,

$$\Pr(\uparrow\uparrow) = |\langle\uparrow\uparrow|\psi\rangle|^2 = \mathrm{Tr}\left[P_{\uparrow\uparrow}\rho\right], \quad P_{\uparrow\uparrow} = P_\uparrow \otimes P_\uparrow. \tag{254}$$

- Consider the following density matrices:

$$\rho_p = |\uparrow\uparrow\rangle\langle\uparrow\uparrow| \quad (\text{pure } \textbf{product state}), \tag{255}$$

$$\rho_m = \frac{1}{2}|\uparrow\uparrow\rangle\langle\uparrow\uparrow| + \frac{1}{2}|\downarrow\downarrow\rangle\langle\downarrow\downarrow| \quad (\textbf{mixed state}), \tag{256}$$

$$\rho_e = |\Phi^+\rangle\langle\Phi^+| = \frac{|\uparrow\uparrow\rangle + |\downarrow\downarrow\rangle}{\sqrt{2}}\frac{\langle\uparrow\uparrow| + \langle\downarrow\downarrow|}{\sqrt{2}} \quad (\text{pure } \textbf{Bell state}). \tag{257}$$

Same “correlation” that “if spin A is up, then spin B is also up”?

- Measurement of spins (z axis)

  – For ρ_p: since $|\psi\rangle = |\uparrow\uparrow\rangle$,

$$\Pr(\uparrow\uparrow) = |\langle\uparrow\uparrow|\uparrow\uparrow\rangle|^2 = 1, \quad \Pr(\uparrow\downarrow) = |\langle\uparrow\downarrow|\uparrow\uparrow\rangle|^2 = 0, \quad \cdots \tag{258}$$

  – For ρ_m:

$$\Pr(\uparrow\uparrow) = \mathrm{Tr}\left[P_{\uparrow\uparrow}\rho_m\right] = \langle\uparrow\uparrow|\left(\frac{1}{2}|\uparrow\uparrow\rangle\langle\uparrow\uparrow| + \frac{1}{2}|\downarrow\downarrow\rangle\langle\downarrow\downarrow|\right)|\uparrow\uparrow\rangle = \frac{1}{2}, \tag{259}$$

$$\Pr(\uparrow\downarrow) = \mathrm{Tr}\left[P_{\uparrow\downarrow}\rho_m\right] = \langle\uparrow\downarrow|\left(\frac{1}{2}|\uparrow\uparrow\rangle\langle\uparrow\uparrow| + \frac{1}{2}|\downarrow\downarrow\rangle\langle\downarrow\downarrow|\right)|\uparrow\downarrow\rangle = 0, \quad \cdots \tag{260}$$

– For ρ_e: since $|\psi\rangle = |\Phi^+\rangle$,

$$\Pr(\uparrow\uparrow) = |\langle\uparrow\uparrow|\Phi^+\rangle|^2 = \left|\frac{1}{\sqrt{2}}\right|^2 = \frac{1}{2}, \quad \Pr(\uparrow\downarrow) = |\langle\uparrow\downarrow|\Phi^+\rangle|^2 = 0, \quad \cdots \tag{261}$$

- Measurement of spins (x **axis**)

– For ρ_p: from Eq. (187),

$$|{+}{+}\rangle = \left(\frac{|\uparrow\rangle + |\downarrow\rangle}{\sqrt{2}}\right) \otimes \left(\frac{|\uparrow\rangle + |\downarrow\rangle}{\sqrt{2}}\right) = \frac{1}{2}\left(|\uparrow\uparrow\rangle + |\uparrow\downarrow\rangle + |\downarrow\uparrow\rangle + |\downarrow\downarrow\rangle\right), \tag{262}$$

which gives

$$\Pr(++) = |\langle{+}{+}|\uparrow\uparrow\rangle|^2 = \left|\frac{1}{2}\right|^2 = \frac{1}{4}, \tag{263}$$

$$\Pr(+-) = |\langle{+}{-}|\uparrow\uparrow\rangle|^2 = \left|\frac{1}{2}\right|^2 = \frac{1}{4}, \quad \cdots \tag{264}$$

– For ρ_m:

$$\begin{aligned} \Pr(++) &= \mathrm{Tr}\left[P_{++}\rho_m\right] = \langle{+}{+}|\left(\frac{1}{2}|\uparrow\uparrow\rangle\langle\uparrow\uparrow| + \frac{1}{2}|\downarrow\downarrow\rangle\langle\downarrow\downarrow|\right)|{+}{+}\rangle \\ &= \frac{1}{2}\frac{1}{2}\frac{1}{2} + \frac{1}{2}\frac{1}{2}\frac{1}{2} = \frac{1}{4}, \quad \cdots \end{aligned} \tag{265}$$

– For ρ_e:

$$|\Phi^+\rangle = \frac{|\uparrow\uparrow\rangle + |\downarrow\downarrow\rangle}{\sqrt{2}} = \frac{1}{\sqrt{2}}\begin{pmatrix}1\\0\\0\\1\end{pmatrix}, \tag{266}$$

$$\begin{aligned} \frac{|{+}{+}\rangle + |{-}{-}\rangle}{\sqrt{2}} &= \frac{1}{\sqrt{2}}\begin{pmatrix} 1/\sqrt{2}\begin{pmatrix}1/\sqrt{2}\\1/\sqrt{2}\end{pmatrix} \\ 1/\sqrt{2}\begin{pmatrix}1/\sqrt{2}\\1/\sqrt{2}\end{pmatrix}\end{pmatrix} + \frac{1}{\sqrt{2}}\begin{pmatrix} 1/\sqrt{2}\begin{pmatrix}1/\sqrt{2}\\-1/\sqrt{2}\end{pmatrix} \\ -1/\sqrt{2}\begin{pmatrix}1/\sqrt{2}\\-1/\sqrt{2}\end{pmatrix}\end{pmatrix} \\ &= \frac{1}{\sqrt{2}}\begin{pmatrix}1/2+1/2\\1/2-1/2\\1/2-1/2\\1/2+1/2\end{pmatrix} = \frac{1}{\sqrt{2}}\begin{pmatrix}1\\0\\0\\1\end{pmatrix} = |\Phi^+\rangle\,. \end{aligned} \tag{267}$$

Namely, **$|\Phi^+\rangle$ is also a Bell state in the x basis**. Therefore,

$$\rho_e = \left(\frac{|{+}{+}\rangle + |{-}{-}\rangle}{\sqrt{2}}\right)\left(\frac{\langle{+}{+}| + \langle{-}{-}|}{\sqrt{2}}\right). \tag{268}$$

Replacing $(\uparrow, \downarrow) \leftrightarrow (+, -)$, the calculation is identical to that in the z basis:

$$\Pr(++) = \Pr(\uparrow\uparrow) = \frac{1}{2}, \quad \Pr(+-) = \Pr(\uparrow\downarrow) = 0, \quad \cdots \tag{269}$$

Table 2: Probabilities of spin-measurement outcomes for the density matrices ρ_p, ρ_m, and ρ_e.

density matrix	$\uparrow\uparrow$	$\uparrow\downarrow$	$\downarrow\uparrow$	$\downarrow\downarrow$	$++$	$+-$	$-+$	$--$
ρ_p	1	0	0	0	1/4	1/4	1/4	1/4
ρ_m	1/2	0	0	1/2	1/4	1/4	1/4	1/4
ρ_e	1/2	0	0	1/2	1/2	0	0	1/2

- Summary (Table 2)
  - ρ_p: spins aligned only when both are **up along the z axis**, s_x are completely random
  - ρ_m: spins aligned for both **up and down along the z axis**, s_x are completely random
    Observing $|\uparrow_A\rangle$ determines $|\uparrow_B\rangle$, while observing $|+_A\rangle$ leaves spin B completely random.
  - ρ_e: spins aligned in **all cases**, both x and z directions
    Observing $|\uparrow_A\rangle$ determines $|\uparrow_B\rangle$, and observing $|+_A\rangle$ determines $|+_B\rangle$.

- Difference between ρ_m and ρ_e:

$$\begin{aligned}\rho_e &= \frac{1}{2}|\uparrow\uparrow\rangle\langle\uparrow\uparrow| + \frac{1}{2}|\uparrow\uparrow\rangle\langle\downarrow\downarrow| + \frac{1}{2}|\downarrow\downarrow\rangle\langle\uparrow\uparrow| + \frac{1}{2}|\downarrow\downarrow\rangle\langle\downarrow\downarrow| \\ &= \rho_m \underbrace{+\frac{1}{2}|\uparrow\uparrow\rangle\langle\downarrow\downarrow| + \frac{1}{2}|\downarrow\downarrow\rangle\langle\uparrow\uparrow|}_{\text{interference terms}}.\end{aligned} \tag{270}$$

ρ_e: a **coherent** superposition with complex coefficients: **quantum correlations**.

ρ_m: a probabilistic mixture of density matrices with real weights: classical correlations

10.3 Entanglement and reduced density matrices

- If ρ is a pure **product state**, then ρ_A is also a pure state:

$$\rho = \Big(|\psi\rangle \otimes |\phi\rangle\Big)\Big(\langle\psi| \otimes \langle\phi|\Big) = |\psi\rangle\langle\psi| \otimes |\phi\rangle\langle\phi|, \tag{271}$$

$$\rho_A = \mathrm{Tr}_B[\rho] = |\psi\rangle\langle\psi| \, \mathrm{Tr}[|\phi\rangle\langle\phi|] = |\psi\rangle\langle\psi|. \tag{272}$$

For $\rho_p = |\uparrow\uparrow\rangle\langle\uparrow\uparrow| = |\uparrow\rangle\langle\uparrow| \otimes |\uparrow\rangle\langle\uparrow|$, substituting $\alpha = 1$, $\beta = \gamma = \delta = 0$ into Eq. (223) gives,

$$\rho_A = \begin{pmatrix} 1 & 0 \\ 0 & 0 \end{pmatrix} = |\uparrow\rangle\langle\uparrow|. \tag{273}$$

- If ρ is an **entangled pure state**, then ρ_A **is a mixed state**.
  For $\rho_e = |\Phi^+\rangle \langle\Phi^+|$, substituting $\alpha = \delta = 1/\sqrt{2}$, $\beta = \gamma = 0$ into Eq. (223) gives,

$$\rho_A = \begin{pmatrix} \frac{1}{2} & 0 \\ 0 & \frac{1}{2} \end{pmatrix} = \frac{1}{2} |\uparrow\rangle \langle\uparrow| + \frac{1}{2} |\downarrow\rangle \langle\downarrow| \,. \tag{274}$$

- Even when ρ is in a pure state, ρ_A can be a mixed state.
  Conversely, every mixed state can be regarded as ρ_A **of a pure state** in a larger Hilbert space (**purification**).

- The linear entropy measures the deviation of the **purity of** ρ_A from unity (a pure state):

$$\mathcal{E} = 1 - \mathrm{Tr}\left[\rho_A^2\right] . \tag{275}$$

11 Bell's inequality

11.1 EPR pair and spin correlation

- EPR (Einstein–Podolsky–Rosen) pair:

$$|\Psi^-\rangle = \frac{|\uparrow\downarrow\rangle - |\downarrow\uparrow\rangle}{\sqrt{2}}. \tag{276}$$

  Bell state with total spin zero

- The probabilities of obtaining $|\uparrow\rangle$ and $|\downarrow\rangle$ by **measuring only spin A** are equal:

$$\Pr(\uparrow_A) = \mathrm{Tr}\left[\, |\uparrow\rangle\langle\uparrow| \rho_A\right] = \frac{1}{2}, \quad \Pr(\downarrow_A) = \mathrm{Tr}\left[\, |\downarrow\rangle\langle\downarrow| \rho_A\right] = \frac{1}{2}. \tag{277}$$

- If $|\uparrow\rangle$ is observed, the wave function collapses to,

$$|\Psi^-\rangle \to |\uparrow\downarrow\rangle\,, \tag{278}$$

  so the **unmeasured spin B is determined** to be $|\downarrow\rangle$.

- Measurement fixes the state (a superposition before the measurement as Schrödinger's cat).

- Quantum correlation is preserved even when spins A and B are spatially separated.

- Einstein–Podolsky–Rosen [55]: counterintuitive?
  Locality: an operation at one location cannot influence a distant system.
  Physical reality: physical quantities have definite values before measurement.

- **Spin correlation function**: for unit vectors $\boldsymbol{n}$ and $\boldsymbol{m}$,

$$C(\boldsymbol{n}, \boldsymbol{m}) = \langle\Psi^-|\boldsymbol{n}\cdot\boldsymbol{\sigma}\otimes\boldsymbol{m}\cdot\boldsymbol{\sigma}|\Psi^-\rangle = n_i m_j \langle\Psi^-|\sigma_i\otimes\sigma_j|\Psi^-\rangle\,. \tag{279}$$

  Expectation value of measuring spin A along $\boldsymbol{n}$ and spin B along $\boldsymbol{m}$ (Fig. 22, left).

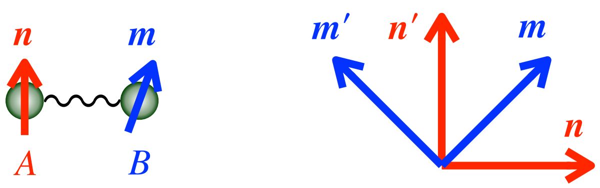

Figure 22: Left: schematic illustration of the spin correlation function. Right: measurement axes that maximize the CHSH correlation in Eq. (294).

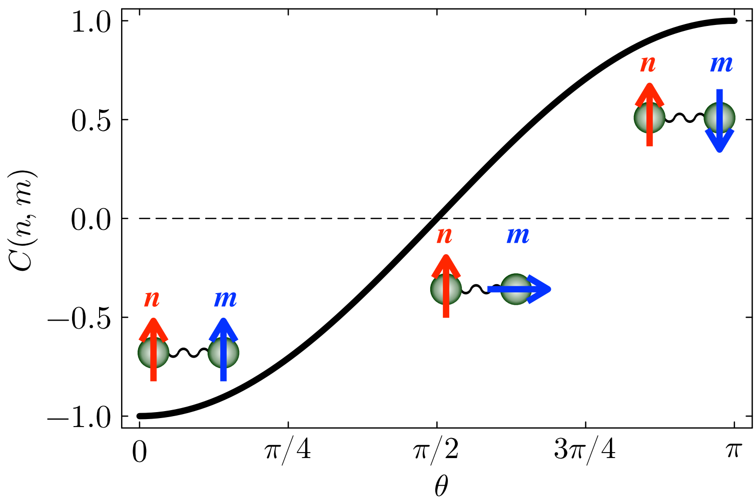

Figure 23: Spin correlation function $C(\boldsymbol{n},\boldsymbol{m})$ in Eq. (281).

- Since $|\Psi^-\rangle$ has total spin zero,

$$\begin{aligned}(\sigma_i \otimes 1 + 1 \otimes \sigma_i)\,|\Psi^-\rangle &= 0 \\ \sigma_i \otimes 1\,|\Psi^-\rangle &= -1 \otimes \sigma_i\,|\Psi^-\rangle\,. \end{aligned} \tag{280}$$

The correlation function is determined by the angle θ between $\boldsymbol{n}$ and $\boldsymbol{m}$:

$$\begin{aligned} C(\boldsymbol{n},\boldsymbol{m}) &= -n_i m_j \langle\Psi^-|\sigma_i\sigma_j \otimes 1|\Psi^-\rangle \\ &= -n_i m_j \langle\Psi^-|(\delta_{ij} + i\epsilon_{ijk}\sigma_k) \otimes 1|\Psi^-\rangle \\ &= -\boldsymbol{n}\cdot\boldsymbol{m} \\ &= -\cos\theta. \end{aligned} \tag{281}$$

- $C(\boldsymbol{n},\boldsymbol{m}) = 1$ for antiparallel axes, 0 for perpendicular axes, and -1 for parallel axes (Fig. 23). Since $|\Psi^-\rangle$ always consists of antiparallel spins, the correlation is maximal at $\theta = \pi$.

11.2 Hidden variable theory

- Locally realistic theory with an unknown parameter λ and a probability distribution $\rho(\lambda)$
- Expectation value of an observable O is given by

$$\langle O\rangle_{\rm HV} = \int d\lambda\,\rho(\lambda)O(\lambda), \qquad \int d\lambda\,\rho(\lambda) = 1. \tag{282}$$

$\to \rho(\lambda)$ plays a role of the density matrix ρ.

The distribution is chosen so that the **expectation value agrees** with quantum mechanics:

$$\langle O\rangle_{\rm HV} = \underbrace{\mathrm{Tr}\,[O\rho]}_{\text{Quantum mechanics}}\,. \tag{283}$$

- The measurement outcome is predetermined.
  The probabilistic nature $\leftarrow$ unknown variable λ

- Spin correlation,

$$C(\boldsymbol{n}, \boldsymbol{m})_{\mathrm{HV}} = \int d\lambda\, \rho(\lambda) N(\boldsymbol{n}, \lambda) M(\boldsymbol{m}, \lambda). \tag{284}$$

  $N(\boldsymbol{n}, \lambda) \in \{1, -1\}$: outcome of a single measurement (fixed λ) of spin A along the $\boldsymbol{n}$ axis

- With suitable choice of distributions, $C(\boldsymbol{n}, \boldsymbol{m})_{\mathrm{HV}} = C(\boldsymbol{n}, \boldsymbol{m})$ for **two axes** $\{\boldsymbol{n}, \boldsymbol{m}\}$.

- When $\boldsymbol{n} = \boldsymbol{m}$, Eq. (281) gives $C(\boldsymbol{n}, \boldsymbol{n}) = -1$. Therefore,

$$C(\boldsymbol{n}, \boldsymbol{n})_{\mathrm{HV}} = \int d\lambda\, \rho(\lambda) N(\boldsymbol{n}, \lambda) M(\boldsymbol{n}, \lambda) = -1. \tag{285}$$

  Since $N(\boldsymbol{n}, \lambda) M(\boldsymbol{n}, \lambda) = \pm 1$ for every λ, this is possible only if

$$N(\boldsymbol{n}, \lambda) = -M(\boldsymbol{n}, \lambda) \qquad \text{(perfectly anticorrelated, c.f., Eq. (280))}. \tag{286}$$

- Bell's inequality [57]: for correlations involving **three or more axes**, the predictions of quantum mechanics and hidden variable theory differ.
  (Equivalently, quantum mechanics cannot be described by a single $\rho(\lambda)$.)

11.3 CHSH inequality

- Extension of Bell's inequality by Clauser, Horne, Shimony, and Holt (CHSH) [56].

- Choose two measurement axes for each spin:

$$\text{spin } A : \boldsymbol{n}, \boldsymbol{n}', \tag{287}$$
$$\text{spin } B : \boldsymbol{m}, \boldsymbol{m}'. \tag{288}$$

- CHSH correlation: a combination of four spin correlations,

$$S = C(\boldsymbol{n}, \boldsymbol{m}) - C(\boldsymbol{n}, \boldsymbol{m}') + C(\boldsymbol{n}', \boldsymbol{m}) + C(\boldsymbol{n}', \boldsymbol{m}'). \tag{289}$$

- **CHSH inequality**: in a hidden variable theory (local realism),

$$0 \leq |S| \leq 2. \tag{290}$$

- Let $s(\lambda)$ be the contribution from a single measurement:

$$\begin{aligned} s(\lambda) &= NM - NM' + N'M + N'M' \\ &= N(M - M') + N'(M + M'). \end{aligned} \tag{291}$$

  Since each measurement outcome is ± 1, there are four possible combinations for M and M':

M	M'	$M-M'$	$M+M'$	$s(\lambda)$
1	1	0	2	$2N'$
1	-1	2	0	$2N$
-1	1	-2	0	$-2N$
-1	-1	0	-2	$-2N'$

Since N and N' also take only the values ± 1,

$$s(\lambda) = \pm 2. \tag{292}$$

The maximum and minimum values of a single measurement are $+2$ and -2.

- Average over all measurements,

$$S = \int d\lambda\, \rho(\lambda)\, s(\lambda), \tag{293}$$

must lie between the maximum and minimum values → Eq. (290).

- In quantum mechanics, choosing the measurement axes as shown in Fig. 22 (right),

$$\begin{aligned} S &= -(\cos\theta_{nm} - \cos\theta_{nm'} + \cos\theta_{n'm} + \cos\theta_{n'm'}) \\ &= -\left(\cos\frac{\pi}{4} - \cos\frac{3\pi}{4} + \cos\frac{\pi}{4} + \cos\frac{\pi}{4}\right) \\ &= -\left(\frac{1}{\sqrt{2}} - (-\frac{1}{\sqrt{2}}) + \frac{1}{\sqrt{2}} + \frac{1}{\sqrt{2}}\right) \\ &= -2\sqrt{2}, \end{aligned} \tag{294}$$

which violates the CHSH inequality (290).

11.4 Experimental tests

- Tests using **photon** pairs [58]
  - Photon pairs produced in a Ca cascade decay
  - Measure the polarization correlation between the emitted photons.
  - Bell's inequality is violated, in agreement with the prediction of quantum mechanics.
  - Several experimental **loopholes** were identified, leading to continual improvements.

- Tests using **proton** pairs [59]
  - A deuteron (d) beam is incident on a liquid hydrogen (^{1}H) target:

$$^1\mathrm{H}(d, {}^2\mathrm{He})n. \tag{295}$$

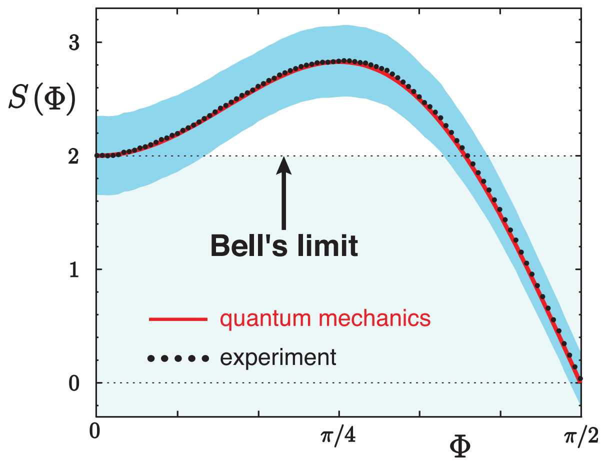

Figure 24: Spin correlation of a proton pair. Adapted from Ref. [59].

- "^{2}He": a low-energy pp pair in the spin-singlet state (see Sec. 13).
  A smaller relative momentum gives a higher spin-correlation purity.
- The proton spins in the final state are measured through rescattering.
  A larger proton momentum improves the polarization analyzing power.
- The reaction (295) produces pp pairs with small relative momentum but large total momentum (i.e., each proton has a large momentum).
- Result: the experimental data (black dots in Fig. 24) agree well with the quantum-mechanical prediction (red solid curve in Fig. 24).

12 Entanglement power of the S matrix

12.1 S matrix and s-wave scattering

- **S matrix**: **operator** that transforms initial state into final state in scattering

$$|\text{out}\rangle = S\,|\text{in}\rangle\,. \tag{296}$$

- Elastic scattering: characterized by momentum p and scattering angle θ
  Partial wave decomposition: scattering is described as a function of p for each ℓ (§3).

- In the following, consider only the s-wave ($\ell = 0$), which is dominant at low energies:

$$s(p) = e^{2i\delta(p)}. \tag{297}$$

  The **scattering phase shift** δ is a function of p.
  Same S matrix for δ and $\delta + n\pi$ ($n \in \mathbb{Z}$): physically equivalent

- Differential cross section and scattering amplitude:

$$\frac{d\sigma}{d\Omega} = |f(p)|^2, \quad f(p) = \frac{1}{p\cot\delta - ip}. \tag{298}$$

  The phase shift contains all the information about the scattering.

- **Scattering length** a: characterizes the low-energy scattering (§4.5):

$$-\frac{1}{a} = \lim_{p\to 0}[p\cot\delta]. \tag{299}$$

  Note that $\delta \to 0$ as $p \to 0$, and a can be either positive or negative.

- Low-energy limit of the total cross section:

$$\lim_{p\to 0}\sigma(p) = 4\pi a^2, \quad \sigma(p) = \int d\Omega\,|f(p)|^2. \tag{300}$$

12.2 Scattering length and symmetry

- The unitarity bound (42) $\leftarrow$ unitarity of the S matrix:

$$\sigma(p) \le \frac{4\pi}{p^2}. \tag{301}$$

  As $p \to 0$, the upper bound of the cross section diverges.
  $\Rightarrow$ The magnitude of the scattering length $|a_0|$ can take any value from 0 to ∞.

- $|a| \to \infty$: the unitarity bound is saturated in the limit $p \to 0$ (**unitary limit**).

- Feshbach resonance in cold atoms (§5): a is controlled by external magnetic field
- Near the unitary limit, low-energy universality emerges [44, 60].
  Ex) when a is large and positive, a shallow bound state exists with (see Eq. (76))

$$B = \frac{1}{2\mu a^2}. \tag{302}$$

  Binding energy B is determined solely by a.

- Much larger $|a|$ than the typical length scale → **scale invariance**:

$$\begin{aligned} a = 0 \quad &: \text{ noninteracting for } p \to 0, \\ |a| \to \infty \quad &: \text{ infinitely strong interaction for } p \to 0 \text{ (unitary limit)}. \end{aligned}$$

- In nonrelativistic systems, scale invariance → **nonrelativistic conformal symmetry** [10].
- The largest symmetry of the free Schrödinger equation (spacetime translations, rotations, Galilean boosts, scale transformations, and special conformal transformations)

12.3 Quantum gates in two-spin system

- State is transformed by an operator (**quantum gate**) U:

$$|\phi\rangle = U\,|\psi\rangle\,. \tag{303}$$

- Controlled-NOT (**CNOT**) gate:

$$\begin{aligned} \mathrm{CNOT} &= P_\uparrow \otimes 1 + P_\downarrow \otimes \sigma_x \\ &= \begin{pmatrix} 1 & 0 \\ 0 & 0 \end{pmatrix} \otimes \begin{pmatrix} 1 & 0 \\ 0 & 1 \end{pmatrix} + \begin{pmatrix} 0 & 0 \\ 0 & 1 \end{pmatrix} \otimes \begin{pmatrix} 0 & 1 \\ 1 & 0 \end{pmatrix} = \begin{pmatrix} 1 & 0 & 0 & 0 \\ 0 & 1 & 0 & 0 \\ 0 & 0 & 0 & 1 \\ 0 & 0 & 1 & 0 \end{pmatrix}. \end{aligned} \tag{304}$$

  Action: spin B (target qubit) is flipped when spin A (control qubit) is $|\downarrow\rangle$

$$\mathrm{CNOT}\,|\uparrow\uparrow\rangle = |\uparrow\uparrow\rangle\,, \quad \mathrm{CNOT}\,|\uparrow\downarrow\rangle = |\uparrow\downarrow\rangle\,, \tag{305}$$

$$\mathrm{CNOT}\,|\downarrow\uparrow\rangle = |\downarrow\downarrow\rangle\,, \quad \mathrm{CNOT}\,|\downarrow\downarrow\rangle = |\downarrow\uparrow\rangle\,, \tag{306}$$

$$\mathrm{CNOT}\begin{pmatrix} \alpha \\ \beta \\ \gamma \\ \delta \end{pmatrix} = \begin{pmatrix} \alpha \\ \beta \\ \delta \\ \gamma \end{pmatrix}. \tag{307}$$

- **SWAP** gate:

$$\text{SWAP} = \frac{1 + \boldsymbol{\sigma}_A \cdot \boldsymbol{\sigma}_B}{2} = \frac{1}{2}\left(1 + \sum_i \sigma_i \otimes \sigma_i\right) = \begin{pmatrix} 1 & 0 & 0 & 0 \\ 0 & 0 & 1 & 0 \\ 0 & 1 & 0 & 0 \\ 0 & 0 & 0 & 1 \end{pmatrix}. \tag{308}$$

  Action: exchanges spins A and B

$$\text{SWAP}\,|{\uparrow\uparrow}\rangle = |{\uparrow\uparrow}\rangle\,, \quad \text{SWAP}\,|{\uparrow\downarrow}\rangle = |{\downarrow\uparrow}\rangle\,, \tag{309}$$

$$\text{SWAP}\,|{\downarrow\uparrow}\rangle = |{\uparrow\downarrow}\rangle\,, \quad \text{SWAP}\,|{\downarrow\downarrow}\rangle = |{\downarrow\downarrow}\rangle\,, \tag{310}$$

$$\text{SWAP}\begin{pmatrix} \alpha \\ \beta \\ \gamma \\ \delta \end{pmatrix} = \begin{pmatrix} \alpha \\ \gamma \\ \beta \\ \delta \end{pmatrix}. \tag{311}$$

- Representation in terms of CNOT (Fig. 25):
  CNOT gate with spin B as the control qubit is,

$$1 \otimes P_\uparrow + \sigma_x \otimes P_\downarrow = \begin{pmatrix} 1 & 0 & 0 & 0 \\ 0 & 0 & 0 & 1 \\ 0 & 0 & 1 & 0 \\ 0 & 1 & 0 & 0 \end{pmatrix}, \tag{312}$$

  and therefore,

$$\begin{aligned} \begin{pmatrix} 1 & 0 & 0 & 0 \\ 0 & 1 & 0 & 0 \\ 0 & 0 & 0 & 1 \\ 0 & 0 & 1 & 0 \end{pmatrix} \begin{pmatrix} 1 & 0 & 0 & 0 \\ 0 & 0 & 0 & 1 \\ 0 & 0 & 1 & 0 \\ 0 & 1 & 0 & 0 \end{pmatrix} \begin{pmatrix} 1 & 0 & 0 & 0 \\ 0 & 1 & 0 & 0 \\ 0 & 0 & 0 & 1 \\ 0 & 0 & 1 & 0 \end{pmatrix} &= \begin{pmatrix} 1 & 0 & 0 & 0 \\ 0 & 1 & 0 & 0 \\ 0 & 0 & 0 & 1 \\ 0 & 0 & 1 & 0 \end{pmatrix} \begin{pmatrix} 1 & 0 & 0 & 0 \\ 0 & 0 & 1 & 0 \\ 0 & 0 & 0 & 1 \\ 0 & 1 & 0 & 0 \end{pmatrix} \\ &= \begin{pmatrix} 1 & 0 & 0 & 0 \\ 0 & 0 & 1 & 0 \\ 0 & 1 & 0 & 0 \\ 0 & 0 & 0 & 1 \end{pmatrix} = \text{SWAP}. \end{aligned} \tag{313}$$

  Any two-qubit gate can be constructed from arbitrary single-qubit gates and CNOT gates

- Change of **entanglement**:

$$\begin{cases} \text{CNOT}\,|{\uparrow\uparrow}\rangle = |{\uparrow\uparrow}\rangle\,, & \text{entanglement remains zero,} \\ \text{CNOT}\,|{+\uparrow}\rangle = |\Phi^+\rangle\,, & \text{entanglement changes from zero to maximal,} \\ \text{CNOT}\,|\Phi^+\rangle = |{+\uparrow}\rangle\,, & \text{entanglement changes from maximal to zero.} \end{cases} \tag{314}$$

  Quantum gates can either increase or decrease entanglement.
  The change depends on the input state.

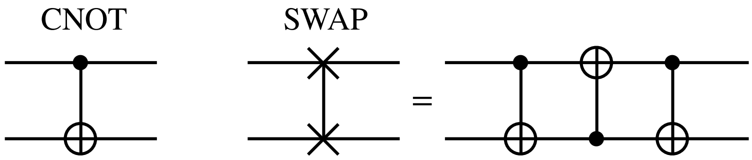

Figure 25: Quantum circuit representation of two-qubit gates. Left: controlled-NOT (CNOT) gate. Right: SWAP gate.

12.4 Entanglement power

- **Entanglement power** (EP): ability of an operator U to **generate** entanglement [61]

$$E(U) = \overline{\mathcal{E}\big(U\,|\text{product state}\rangle\big)}. \tag{315}$$

  Average over initial product states

- Initial product state:

$$\mathcal{E}\big(|\text{product state}\rangle\big) = 0, \tag{316}$$
$$\Rightarrow \quad \mathcal{E}\big(U\,|\text{product state}\rangle\big) = \text{the entanglement generated by } U. \tag{317}$$

- Average is taken over **all possible** initial product states
  $\leftarrow$ **state independent** definition of EP

- Representation of product states on the Bloch sphere [62]:

$$|\theta_A,\phi_A\rangle\otimes|\theta_B,\phi_B\rangle = \begin{pmatrix}\cos\frac{\theta_A}{2}\\ \sin\frac{\theta_A}{2}e^{i\phi_A}\end{pmatrix}\otimes\begin{pmatrix}\cos\frac{\theta_B}{2}\\ \sin\frac{\theta_B}{2}e^{i\phi_B}\end{pmatrix} = \begin{pmatrix}\cos\frac{\theta_A}{2}\cos\frac{\theta_B}{2}\\ \cos\frac{\theta_A}{2}\sin\frac{\theta_B}{2}e^{i\phi_B}\\ \sin\frac{\theta_A}{2}\cos\frac{\theta_B}{2}e^{i\phi_A}\\ \sin\frac{\theta_A}{2}\sin\frac{\theta_B}{2}e^{i(\phi_A+\phi_B)}\end{pmatrix}. \tag{318}$$

  The directions of spins A and B are specified by (θ_A,ϕ_A) and (θ_B,ϕ_B), respectively.

- The angles (θ,ϕ) cover the entire solid angle:

$$\int d\Omega = \int_0^{\pi}\sin\theta\,d\theta\int_0^{2\pi}d\phi = \int_{-1}^{1}d(\cos\theta)\int_0^{2\pi}d\phi = 4\pi. \tag{319}$$

- Explicit expression for the EP:

$$\begin{aligned}E(U) &= \int\frac{d\Omega_A}{4\pi}\int\frac{d\Omega_B}{4\pi}\mathcal{E}\big(U\,|\theta_A,\phi_A\rangle\otimes|\theta_B,\phi_B\rangle\big)\\ &= 1-\int\frac{d\Omega_A}{4\pi}\int\frac{d\Omega_B}{4\pi}\mathrm{Tr}_A\left[\rho_A^2\right],\end{aligned} \tag{320}$$

where

$$\rho_A = \mathrm{Tr}_B \left[U \big(|\theta_A, \phi_A\rangle \otimes |\theta_B, \phi_B\rangle \big) \big(\langle\theta_A, \phi_A| \otimes \langle\theta_B, \phi_B| \big) U^\dagger \right]. \tag{321}$$

For a given U, EP is calculated by this equation.

- If U is the S matrix, the EP depends on the scattering phase shift δ (§13.3).
- Any **nonlocal** two-spin operator U can be characterized by three parameters β_a:

$$U = \exp\left\{ i \sum_a \beta_a \sigma_a \otimes \sigma_a \right\} \quad (a = 1, 2, 3). \tag{322}$$

$\leftarrow$ Cartan decomposition of SU(4)/(SU(2) $\times$ SU(2)) [62]

- EP of U can be given by β_a as,

$$E(U) = \frac{1}{6} - \frac{1}{18} \sum_{a<b} \cos(4\beta_a)\cos(4\beta_b). \tag{323}$$

13 Nuclear force and entanglement suppression

13.1 Two-nucleon wave function

- Nucleon follows $\mathrm{SU}(2)_S \times \mathrm{SU}(2)_I$ **symmetry**
  - Spin $\mathrm{SU}(2)_S \leftarrow$ Lorentz (Poincaré) symmetry of QCD
  - Isospin $\mathrm{SU}(2)_I \leftarrow$ Isospin symmetry of QCD (interchange of the u and d quarks)

- One-nucleon state:

$$|N\rangle = \psi(\boldsymbol{r}) \otimes |\text{spin}\rangle \otimes |\text{isospin}\rangle . \tag{324}$$

$\psi(\boldsymbol{r})$: Spatial wave function

$|\text{spin}\rangle$: Spin wave function (spin-1/2), $\{|\uparrow\rangle, |\downarrow\rangle\}$

$|\text{isospin}\rangle$: Isospin wave function (isospin-1/2), $\{|p\rangle, |n\rangle\}$

- Two-nucleon system:

$$\text{Spatial part : } \psi(\boldsymbol{r}_A)\psi(\boldsymbol{r}_B) = \Psi(\boldsymbol{R})\phi(\boldsymbol{r}), \quad \boldsymbol{R} = \frac{\boldsymbol{r}_A + \boldsymbol{r}_B}{2}, \quad \boldsymbol{r} = \boldsymbol{r}_A - \boldsymbol{r}_B, \tag{325}$$

$$\text{Spin and isospin : } \frac{1}{2} \otimes \frac{1}{2} = 0 \oplus 1. \tag{326}$$

- Two-nucleon state (center-of-mass frame):

$$|NN\rangle = \phi_\ell(\boldsymbol{r}) \otimes |\text{Spin}\rangle \otimes |\text{Isospin}\rangle . \tag{327}$$

$\phi_\ell(\boldsymbol{r})$: Spatial wave function (relative coordinate $\boldsymbol{r}$, orbital angular momentum ℓ)

$|\text{Spin}\rangle$: Spin wave function: $|S, S_z\rangle = |0,0\rangle, |1,+1\rangle, |1,0\rangle, |1,-1\rangle$

$|\text{Isospin}\rangle$: Isospin wave function: $|I, I_z\rangle = |0,0\rangle, |1,+1\rangle, |1,0\rangle, |1,-1\rangle$

- In the computational basis and the Bell basis:

$$|0,0\rangle = \frac{|\uparrow\downarrow\rangle - |\downarrow\uparrow\rangle}{\sqrt{2}} = |\Psi^-\rangle , \quad |1,0\rangle = \frac{|\uparrow\downarrow\rangle + |\downarrow\uparrow\rangle}{\sqrt{2}} = |\Psi^+\rangle , \tag{328}$$

$$|1,+1\rangle = |\uparrow\uparrow\rangle = \frac{|\Phi^+\rangle + |\Phi^-\rangle}{\sqrt{2}}, \quad |1,-1\rangle = |\downarrow\downarrow\rangle = \frac{|\Phi^+\rangle - |\Phi^-\rangle}{\sqrt{2}}. \tag{329}$$

13.2 Symmetries of the nuclear force

- Spatial exchange operator P_r: Exchange of the two nucleons ($\boldsymbol{r}_A \leftrightarrow \boldsymbol{r}_B$), namely, $\boldsymbol{r} \to -\boldsymbol{r}$. Using the property of the spherical harmonics,

$$P_r\phi_\ell(\boldsymbol{r}) = \phi_\ell(-\boldsymbol{r}) = (-1)^\ell \phi_\ell(\boldsymbol{r}). \tag{330}$$

$\phi_\ell(\boldsymbol{r})$ is **symmetric** (eigenvalue $+1$) for even ℓ, **antisymmetric** (eigenvalue -1) for odd ℓ.

Table 3: Spin and isospin of the s-wave two-nucleon states.

Orbital angular momentum	Spin	Isospin
$\ell = 0$ (symmetric)	$S = 0$ (antisymmetric)	$I = 1$ (symmetric)
	$S = 1$ (symmetric)	$I = 0$ (antisymmetric)

- Eigenvalues of $\boldsymbol{\sigma}_A \cdot \boldsymbol{\sigma}_B$

$$\boldsymbol{\sigma}_A \cdot \boldsymbol{\sigma}_B \,|0,0\rangle = -3\,|0,0\rangle\,, \quad \boldsymbol{\sigma}_A \cdot \boldsymbol{\sigma}_B \,|1,S_z\rangle = +1\,|1,S_z\rangle\,. \tag{331}$$

- Spin exchange operator (SWAP gate in Eq. (308)):

$$P_\sigma = \frac{1 + \boldsymbol{\sigma}_A \cdot \boldsymbol{\sigma}_B}{2}, \tag{332}$$

$$P_\sigma\,|0,0\rangle = -\,|0,0\rangle\,, \quad P_\sigma\,|1,S_z\rangle = +\,|1,S_z\rangle\,. \tag{333}$$

This operator exchanges the spins of nucleons A and B.
$S = 0$ is **antisymmetric**, $S = 1$ is **symmetric** under the exchange.

- Isospin exchange operator:

$$P_\tau = \frac{1 + \boldsymbol{\tau}_A \cdot \boldsymbol{\tau}_B}{2}, \tag{334}$$

$$P_\tau\,|0,0\rangle = -\,|0,0\rangle\,, \quad P_\tau\,|1,I_z\rangle = +\,|1,I_z\rangle\,. \tag{335}$$

$I = 0$ is **antisymmetric**, $I = 1$ is **symmetric** under the exchange.

- Fermi statistics: $|NN\rangle$ must be **antisymmetric** under

$$P_r P_\sigma P_\tau\,|NN\rangle = -\,|NN\rangle\,. \tag{336}$$

Allowed states for low-energy (Table 3): I is uniquely determined for a fixed S

- Low-energy s-wave scattering is described by **only two channels**:
  - Spin $S = 0$, isospin $I = 1$: ${}^1S_0$
  - Spin $S = 1$, isospin $I = 0$: ${}^3S_1$

Note: under the $\mathrm{SU}(2)_S \times \mathrm{SU}(2)_I$ symmetry, ${}^1S_0$ **and** ${}^3S_1$ **are independent**.

- Scattering lengths of the physical nuclear force [44]:

$$a(S=0) \equiv a_0 \approx -23.76 \text{ fm}, \quad a(S=1) \equiv a_1 \approx 5.42 \text{ fm}. \tag{337}$$

- Typical length scale of the nuclear force:

$$R_{\text{typ}} \sim \frac{1}{m_\pi} \approx 1.43 \text{ fm}. \tag{338}$$

Range of the one-pion-exchange force, the longest-range interaction between hadrons.

- Scattering lengths $\gg R_{\text{typ}}$
$\Rightarrow$ close to the unitary limit, **nonrelativistic conformal symmetry** [10]:

$$|a_0| \gg \frac{1}{m_\pi}, \quad |a_1| \gg \frac{1}{m_\pi}. \tag{339}$$

- **Both** the $S = 0$ and $S = 1$ channels are close to the unitary limit:

$$\frac{1}{|a_0|} \sim \frac{1}{|a_1|} \ll m_\pi. \tag{340}$$

Similarity between $S = 0$ and $S = 1 \Rightarrow$ **spin-flavor SU(4) symmetry** [8, 9].

- One-nucleon states form the fundamental representation of SU(4):

$$\{|p\uparrow\rangle, |p\downarrow\rangle, |n\uparrow\rangle, |n\downarrow\rangle\}. \tag{341}$$

The irreducible decomposition of the two-nucleon states is:

$$\mathbf{4} \otimes \mathbf{4} = \mathbf{6} \oplus \mathbf{10}. \tag{342}$$

${}^1S_0$ (3 isospin states) and ${}^3S_1$ (3 spin states) together form $\mathbf{6}$.

- **Emergent symmetries** cannot be derived directly from QCD.

13.3 Entanglement suppression in the two-nucleon system

- Projection operators onto states with total spin S:

$$\mathcal{J}_0 = \frac{1 - \boldsymbol{\sigma}_A \cdot \boldsymbol{\sigma}_B}{4}, \quad \mathcal{J}_1 = \frac{3 + \boldsymbol{\sigma}_A \cdot \boldsymbol{\sigma}_B}{4}. \tag{343}$$

- pn scattering (isospin is automatically determined from Table 3)

$$S = e^{2i\delta_0}\mathcal{J}_0 + e^{2i\delta_1}\mathcal{J}_1 \propto \frac{3 + e^{-2i(\delta_1-\delta_0)}}{4} + \frac{1 - e^{-2i(\delta_1-\delta_0)}}{4}\boldsymbol{\sigma}_A \cdot \boldsymbol{\sigma}_B. \tag{344}$$

δ_S: phase shift with total spin S.

- Entanglement power (EP) of a general nonlocal operator U:

$$E(U) = \frac{1}{6} - \frac{1}{18}\sum_{a<b}\cos(4\beta_a)\cos(4\beta_b). \tag{345}$$

For $\beta_1 = \beta_2 = \beta_3 = \beta$,

$$E(U) = \frac{1}{6}\sin^2(4\beta), \quad U \propto \frac{3 + e^{-4i\beta}}{4} + \frac{1 - e^{-4i\beta}}{4}\boldsymbol{\sigma}_A \cdot \boldsymbol{\sigma}_B. \tag{346}$$

Comparing Eq. (344) with Eq. (346), we obtain $2\beta = \delta_1 - \delta_0$.

- EP of pn scattering [11, 62]:

$$E(S) = \frac{1}{6}\sin^2[2(\delta_1 - \delta_0)] \geq 0. \tag{347}$$

- The minimum value $E(S) = 0$ is obtained when $\sin[2(\delta_1 - \delta_0)] = 0$:

  - Solution 1: $|\delta_1 - \delta_0| = 0$
  - Solution 2: $|\delta_1 - \delta_0| = \pi/2$

- Solution 1: $S = 0$ and $S = 1$ have the same phase shift
  $\Rightarrow$ **spin-flavor SU(4) symmetry**.

- If Solution 2 is realized in the low-energy limit ($p \to 0$):

$$-\frac{1}{a_0} = \lim_{p\to 0}[p\cot\delta_0], \quad -\frac{1}{a_1} = \lim_{p\to 0}[p\cot\delta_1]. \tag{348}$$

Using $\delta_1 = \delta_0 + \pi/2$ and multiplying the two equations,

$$\frac{1}{a_0}\frac{1}{a_1} = \lim_{p\to 0}\Big[p\cot\delta_0 \cdot p\cot(\delta_0 + \pi/2)\Big] = \lim_{p\to 0}\Big[p^2\cot\delta_0(-\tan\delta_0)\Big] = 0. \tag{349}$$

Either $1/a_0$ or $1/a_1$ must vanish, namely, the **scattering length diverges**.
$\Rightarrow$ **nonrelativistic conformal symmetry**.

13.4 Interpretation in terms of quantum gates

- Interpretation of the solutions [62]

- Solution 1: setting $\delta_1 = \delta_0$,

$$S = e^{2i\delta_0}\mathcal{J}_0 + e^{2i\delta_0}\mathcal{J}_1 = e^{2i\delta_0}(\mathcal{J}_0 + \mathcal{J}_1). \tag{350}$$

Proportional to the **sum** of the projection operators

- Solution 2: setting $\delta_1 = \delta_0 + \pi/2$,

$$S = e^{2i\delta_0}\mathcal{J}_0 + e^{2i(\delta_0+\pi/2)}\mathcal{J}_1 = e^{2i\delta_0}\mathcal{J}_0 + e^{2i\delta_0}e^{i\pi}\mathcal{J}_1 = -e^{2i\delta_0}(\mathcal{J}_1 - \mathcal{J}_0). \tag{351}$$

  Proportional to the **difference** of the projection operators.

- Using the projection operators in Eq. (343),

$$\mathcal{J}_0 + \mathcal{J}_1 = \frac{1 - \boldsymbol{\sigma}_A \cdot \boldsymbol{\sigma}_B}{4} + \frac{3 + \boldsymbol{\sigma}_A \cdot \boldsymbol{\sigma}_B}{4} = 1, \tag{352}$$

$$\mathcal{J}_1 - \mathcal{J}_0 = \frac{3 + \boldsymbol{\sigma}_A \cdot \boldsymbol{\sigma}_B}{4} - \frac{1 - \boldsymbol{\sigma}_A \cdot \boldsymbol{\sigma}_B}{4} = \frac{1 + \boldsymbol{\sigma}_A \cdot \boldsymbol{\sigma}_B}{2} = \text{SWAP}. \tag{353}$$

  Solution 1: S matrix acts as the **identity gate** (identity operator).
  Solution 2: S matrix acts as the **SWAP gate** (spin exchange operator).

- Identity and SWAP **map a product state to another product state**:

$$1\ |\psi_A\rangle \otimes |\psi_B\rangle = |\psi_A\rangle \otimes |\psi_B\rangle\,, \tag{354}$$

$$\text{SWAP}\ |\psi_A\rangle \otimes |\psi_B\rangle = |\psi_B\rangle \otimes |\psi_A\rangle\,. \tag{355}$$

  The output state remains a product state (EE is zero) $\rightarrow$ EP vanishes

- **Only the identity and the SWAP gate** give $E(S) = 0$.
  Indeed, the only solutions of Eq. (345) with vanishing EP are [62],

$$\begin{cases} \beta_1 = \beta_2 = \beta_3 = 0 & \Rightarrow U = 1, \\ \beta_1 = \beta_2 = \beta_3 = \dfrac{\pi}{4} & \Rightarrow U = e^{i\pi/4} \times \text{SWAP}. \end{cases} \tag{356}$$

14 Extension to general spin and flavor

14.1 Spin and flavor of baryons

- Single-quark state

$$|q\rangle = \psi(\boldsymbol{r}) \otimes |\text{color}\rangle \otimes |\text{spin}\rangle \otimes |\text{flavor}\rangle\,. \tag{357}$$

$\psi(\boldsymbol{r})$: Spatial wave function

$|\text{color}\rangle$: Color wave function: $\mathbf{3}$ of SU(3), $\{|r\rangle\,, |g\rangle\,, |b\rangle\}$

$|\text{spin}\rangle$: Spin wave function: spin-1/2 of SU(2), $\{|\uparrow\rangle\,, |\downarrow\rangle\}$

- **Flavor** wave function $|\text{flavor}\rangle$:

$\{|u\rangle\,, |d\rangle\}$: Flavor (isospin) SU(2)

$\{|u\rangle\,, |d\rangle\,, |s\rangle\}$: Flavor SU(3)

- Flavor symmetry is an approximate symmetry ($p \sim uud$, $n \sim udd$, $\Lambda \sim uds$)

$$m_p = 938 \text{ MeV}, \quad m_n = 940 \text{ MeV}, \quad m_\Lambda = 1116 \text{ MeV}. \tag{358}$$

SU(2): valid at the level of a few percent;
SU(3): valid at roughly the 20% level.

- Wave function of a baryon (three-quark state)

$$|qqq\rangle = \phi_\ell(\boldsymbol{\rho}, \boldsymbol{\lambda}) \otimes |\text{Color}\rangle \otimes |\text{Spin}\rangle \otimes |\text{Flavor}\rangle\,. \tag{359}$$

Completely antisymmetric under the exchange of any two quarks.

  - $\phi_\ell(\boldsymbol{\rho}, \boldsymbol{\lambda})$: Jacobi coordinates $\{\boldsymbol{\rho}, \boldsymbol{\lambda}\}$ and total orbital angular momentum ℓ
  - Color wave function $|\text{Color}\rangle$:

$$\mathbf{3} \otimes \mathbf{3} \otimes \mathbf{3} = \mathbf{1} \oplus \mathbf{8} \oplus \mathbf{8} \oplus \mathbf{10}. \tag{360}$$

The completely antisymmetric $\mathbf{1}$ (color confinement):

$$|\text{Color}\rangle = \frac{|rgb\rangle + |brg\rangle + |gbr\rangle - |grb\rangle - |bgr\rangle - |rbg\rangle}{\sqrt{6}}. \tag{361}$$

  - Spin wave function $|\text{Spin}\rangle$:

$$\frac{1}{2} \otimes \frac{1}{2} \otimes \frac{1}{2} = \frac{1}{2} \oplus \frac{1}{2} \oplus \frac{3}{2}. \tag{362}$$

  - Flavor wave function $|\text{Flavor}\rangle$: the same decomposition as Eq. (360)

For the ground state ($\ell = 0$), $|qqq\rangle$ is completely antisymmetric if (Fig. 26):

$$|\text{Spin}\rangle \otimes |\text{Flavor}\rangle = \begin{cases} |S = 1/2\rangle \otimes |\mathbf{8}\rangle & \textbf{Spin-1/2 baryon octet} \\ |S = 3/2\rangle \otimes |\mathbf{10}\rangle & \textbf{Spin-3/2 baryon decuplet} \end{cases}. \tag{363}$$

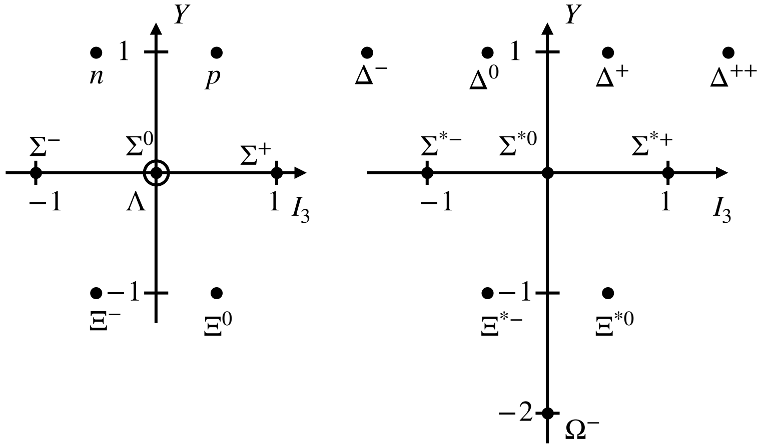

Figure 26: Weight diagrams of the ground-state octet (left) and decuplet (right) baryohns.

14.2 Scattering of octet baryons

- Spin and flavor of the two-octet-baryon system

$$\frac{1}{2}\otimes\frac{1}{2}=\underbrace{0}_{\mathrm{A}}\oplus\underbrace{1}_{\mathrm{S}}, \tag{364}$$

$$\mathbf{8}\otimes\mathbf{8}=\underbrace{\mathbf{1}\oplus\mathbf{8}_S\oplus\mathbf{27}}_{\mathrm{S}}\oplus\underbrace{\mathbf{8}_A\oplus\mathbf{10}\oplus\overline{\mathbf{10}}}_{\mathrm{A}}. \tag{365}$$

For the s wave: spin-A $\otimes$ flavor-S or spin-S $\otimes$ flavor-A

- S matrix: **six independent** scattering channels

$$\begin{aligned} S=&\mathcal{J}_0(\mathcal{F}_{\mathbf{1}}e^{2i\delta_{0,\mathbf{1}}}+\mathcal{F}_{\mathbf{8}_S}e^{2i\delta_{0,\mathbf{8}_S}}+\mathcal{F}_{\mathbf{27}}e^{2i\delta_{0,\mathbf{27}}}) \\ &+\mathcal{J}_1(\mathcal{F}_{\mathbf{8}_A}e^{2i\delta_{1,\mathbf{8}_A}}+\mathcal{F}_{\mathbf{10}}e^{2i\delta_{1,\mathbf{10}}}+\mathcal{F}_{\overline{\mathbf{10}}}e^{2i\delta_{1,\overline{\mathbf{10}}}}). \end{aligned} \tag{366}$$

$\mathcal{J}_S$: projector onto the spin-S state in Eq. (343), $\mathcal{F}_{\boldsymbol{R}}$: flavor projector onto $\boldsymbol{R}$.

- Charge Q and strangeness S conservations: independent scattering in each (Q,S) sector
  Example: $(Q,S)=(+1,0)$: nuclear force (pn scattering), $\delta_{0,\mathbf{27}}$ $({}^1S_0)$ and $\delta_{1,\overline{\mathbf{10}}}$ $({}^3S_1)$

- Sector with the largest number of coupled channels: $(Q,S)=(0,-2)$

$$\Sigma^+\Sigma^-,\ \Sigma^0\Sigma^0,\ \Lambda\Sigma^0,\ \Xi^-p,\ \Xi^0n,\ \Lambda\Lambda. \tag{367}$$

Consequences of entanglement suppression [63]:

$$S\propto 1: \qquad \textbf{Spin-flavor SU(16) symmetry}, \tag{368}$$

$$S\propto \mathrm{SWAP}: \qquad \textbf{Flavor SU(8)} \text{ and } \textbf{NR conformal symmetries}. \tag{369}$$

Enlarged flavor space $\to$ enlarged symmetry
Symmetries of other sectors (e.g. nuclear force) are contained as subgroup symmetries:

$$\mathrm{SU}(16)\supset\mathrm{SU}(4). \tag{370}$$

- Spin-flavor SU(16): symmetry of baryons ($16 = 8 \times 2$)

$$\{|p\uparrow\rangle, |p\downarrow\rangle, |n\uparrow\rangle, |n\downarrow\rangle, |\Lambda\uparrow\rangle, |\Lambda\downarrow\rangle, \cdots\}. \tag{371}$$

c.f.) In the large-N_c limit, spin-flavor SU(6): symmetry of quarks ($6 = 3 \times 2$):

$$\{|u\uparrow\rangle, |u\downarrow\rangle, |d\uparrow\rangle, |d\downarrow\rangle, |s\uparrow\rangle, |s\downarrow\rangle\}. \tag{372}$$

$\Rightarrow$ Entanglement suppression imposes a **stronger constraint than the large-N_c limit** [11]. Lattice QCD indicates evidence for approximate SU(16) symmetry [64].

- In the two-flavor case, both quarks $\{u, d\}$ and baryons $\{p, n\}$ belong to spin-1/2.
$\Rightarrow$ The spin-flavor symmetry is SU(4) for both quarks and baryons.

14.3 Spin-3/2 states

- Spin-3/2 state (4-dimensional qudit): a complex four-component vector

$$|\psi_{\mathbf{4}}\rangle = \begin{pmatrix} a \\ b \\ c \\ d \end{pmatrix}, \quad a, b, c, d \in \mathbb{C}. \tag{373}$$

Without any constraints, there are **eight degrees of freedom** ($\mathcal{H} = \mathbb{C}^4$).
Normalization and phase d.o.f. $\to$ $|\psi_{\mathbf{4}}\rangle$ is described by **six degrees of freedom**.

- Fubini–Study measure on the projective space $\mathbb{C}^4/\!\sim\, = \mathbb{CP}^3$:

$$|\psi_{\mathbf{4}}\rangle = \begin{pmatrix} \cos\theta_1 \sin\theta_2 \sin\theta_3 \\ \sin\theta_1 \sin\theta_2 \sin\theta_3 e^{i\nu_1} \\ \cos\theta_2 \sin\theta_3 e^{i\nu_2} \\ \cos\theta_3 e^{i\nu_3} \end{pmatrix}, \tag{374}$$

$$d\omega_{\mathbf{4}} = \frac{3!}{\pi^3} \prod_{i=1}^{3} d\theta_i d\nu_i \cos\theta_i \sin^{2i-1}\theta_i, \qquad \int d\omega_{\mathbf{4}} = 1. \tag{375}$$

Six degrees of freedom are θ_i, ν_i ($i = 1, 2, 3$).

- Spin operators $\boldsymbol{s}$: 4×4 complex matrices

$$s_x = \begin{pmatrix} 0 & \sqrt{3}/2 & 0 & 0 \\ \sqrt{3}/2 & 0 & 1 & 0 \\ 0 & 1 & 0 & \sqrt{3}/2 \\ 0 & 0 & \sqrt{3}/2 & 0 \end{pmatrix}, \quad s_y = \begin{pmatrix} 0 & -i\sqrt{3}/2 & 0 & 0 \\ i\sqrt{3}/2 & 0 & -i & 0 \\ 0 & i & 0 & -i\sqrt{3}/2 \\ 0 & 0 & i\sqrt{3}/2 & 0 \end{pmatrix}, \tag{376}$$

$$s_z = \begin{pmatrix} 3/2 & 0 & 0 & 0 \\ 0 & 1/2 & 0 & 0 \\ 0 & 0 & -1/2 & 0 \\ 0 & 0 & 0 & -3/2 \end{pmatrix}. \tag{377}$$

- Eigenstates of s_z

$$|\Uparrow\rangle = \begin{pmatrix} 1 \\ 0 \\ 0 \\ 0 \end{pmatrix}, \quad |\uparrow\rangle = \begin{pmatrix} 0 \\ 1 \\ 0 \\ 0 \end{pmatrix}, \quad |\downarrow\rangle = \begin{pmatrix} 0 \\ 0 \\ 1 \\ 0 \end{pmatrix}, \quad |\Downarrow\rangle = \begin{pmatrix} 0 \\ 0 \\ 0 \\ 1 \end{pmatrix}, \tag{378}$$

$$s_z |\Uparrow\rangle = \frac{3}{2} |\Uparrow\rangle, \quad s_z |\uparrow\rangle = \frac{1}{2} |\uparrow\rangle, \quad s_z |\downarrow\rangle = -\frac{1}{2} |\downarrow\rangle, \quad s_z |\Downarrow\rangle = -\frac{3}{2} |\Downarrow\rangle. \tag{379}$$

14.4 Scattering of decuplet baryons

- Spin and flavor of the two-decuplet-baryon system

$$\frac{3}{2} \otimes \frac{3}{2} = \underbrace{0 \oplus 2}_{\text{A}} \oplus \underbrace{1 \oplus 3}_{\text{S}}, \tag{380}$$

$$\mathbf{10} \otimes \mathbf{10} = \underbrace{\mathbf{27} \oplus \mathbf{28}}_{\text{S}} \oplus \underbrace{\overline{\mathbf{10}} \oplus \mathbf{35}}_{\text{A}}. \tag{381}$$

For the s wave: spin-A $\otimes$ flavor-S or spin-S $\otimes$ flavor-A

- S matrix: **eight independent** scattering channels

$$S = \mathcal{J}_0(\mathcal{F}_{\mathbf{27}} e^{2i\delta_{0,\mathbf{27}}} + \mathcal{F}_{\mathbf{28}} e^{2i\delta_{0,\mathbf{28}}}) + \mathcal{J}_1(\mathcal{F}_{\overline{\mathbf{10}}} e^{2i\delta_{1,\overline{\mathbf{10}}}} + \mathcal{F}_{\mathbf{35}} e^{2i\delta_{1,\mathbf{35}}})$$
$$+ \mathcal{J}_2(\mathcal{F}_{\mathbf{27}} e^{2i\delta_{2,\mathbf{27}}} + \mathcal{F}_{\mathbf{28}} e^{2i\delta_{2,\mathbf{28}}}) + \mathcal{J}_3(\mathcal{F}_{\overline{\mathbf{10}}} e^{2i\delta_{3,\overline{\mathbf{10}}}} + \mathcal{F}_{\mathbf{35}} e^{2i\delta_{3,\mathbf{35}}}). \tag{382}$$

- Projection operators for spin-3/2: linear combinations of the quadratic Casimir operator

$$\mathcal{J}_0 = \frac{33}{128} + \frac{31}{96} (\boldsymbol{s}_A \cdot \boldsymbol{s}_B) - \frac{5}{72} (\boldsymbol{s}_A \cdot \boldsymbol{s}_B)^2 - \frac{1}{18} (\boldsymbol{s}_A \cdot \boldsymbol{s}_B)^3, \quad \cdots \tag{383}$$

- (Q,S) conservation: the largest number of coupled channels in $(Q,S)=(0,-2)$

$$\Delta^+\Xi^{*-},\ \Delta^0\Xi^{*0},\ \Sigma^{*0}\Sigma^{*0},\ \Sigma^{*+}\Sigma^{*-}. \tag{384}$$

  Consequences of entanglement suppression [65]:

$$S \propto 1: \quad \textbf{Spin-flavor SU(40) symmetry}, \tag{385}$$

$$S \propto \mathrm{SWAP}: \quad \textbf{Spin SU(4)},\ \textbf{flavor SU(10)},\ \text{and}\ \textbf{NR conformal symmetry}. \tag{386}$$

- Phenomenological application: $\Omega\Omega$ scattering in the $(Q,S)=(-2,-6)$ sector
  Identical particles with no flavor d.o.f.: only antisymmetric $S=0$ and $S=2$ states

- Lattice QCD indicates that the $S=0$ channel is close to the unitary limit [66].

- Entanglement suppression in $\Omega\Omega$ scattering [65] (with proper normalization):

$$S \propto 1_A: \quad \textbf{Spin SU(4) symmetry}, \tag{387}$$

$$S \propto \mathrm{SWAP}_A: \quad \textbf{NR conformal symmetry}. \tag{388}$$

  $\Rightarrow$ Spin-2 channel is either at the unitary limit ($S \propto 1_A$) or weakly interacting ($S \propto \mathrm{SWAP}_A$).

Last Update: August 4, 2026

References

[1] S. Navas *et al.* [Particle Data Group], Phys. Rev. D **110**, 030001 (2024).

[2] N. Brambilla, S. Eidelman, C. Hanhart, A. Nefediev, C. P. Shen, C. E. Thomas, A. Vairo and C. Z. Yuan, Phys. Rept. **873**, 1-154 (2020), arXiv:1907.07583 [hep-ex].

[3] C. Hanhart, arXiv:2504.06043 [hep-ph].

[4] LHCb Collaboration, R. Aaij *et al.*, Phys. Rev. Lett. **115**, 072001 (2015), arXiv:1507.03414 [hep-ex].

[5] LHCb Collaboration, R. Aaij *et al.*, Phys. Rev. Lett. **122**, 222001 (2019), arXiv:1904.03947 [hep-ex].

[6] LHCb Collaboration, R. Aaij *et al.*, Nature Phys. **18**, 751 (2022), arXiv:2109.01038 [hep-ex].

[7] LHCb Collaboration, R. Aaij *et al.*, Nature Commun. **13**, 3351 (2022), arXiv:2109.01056 [hep-ex].

[8] E. Wigner, Phys. Rev. **51**, 106 (1937).

[9] D. B. Kaplan and M. J. Savage, Phys. Lett. B **365**, 244 (1996), hep-ph/9509371.

[10] T. Mehen, I. W. Stewart, and M. B. Wise, Phys. Lett. B **474**, 145 (2000), hep-th/9910025.

[11] S. R. Beane, D. B. Kaplan, N. Klco, and M. J. Savage, Phys. Rev. Lett. **122**, 102001 (2019), arXiv:1812.03138 [nucl-th].

[12] 羽田野直道, 井村健一郎, 非エルミート量子力学 (KS 物理専門書, 2023).

[13] A. Bohm, *Quantum Mechanics: Foundations and Applications, 3rd edition* (Springer, 2001).

[14] N. Moiseyev, *Non-Hermitian Quantum Mechanics* (Cambridge University Press, Cambridge, 2011).

[15] Y. Ashida, Z. Gong, and M. Ueda, Adv. Phys. **69**, 249 (2021), arXiv:2006.01837 [cond-mat.mes-hall].

[16] J. R. Taylor, *Scattering Theory: The Quantum Theory on Nonrelativistic Collisions* (Wiley, New York, 1972).

[17] R. Newton, *Scattering theory of waves and particles, 2nd edition* (Springer, Berlin, 2014).

[18] 永江知文, 兵藤哲雄, K 中間子原子核の物理 (共立出版, 2023).

[19] T. Hyodo and M. Niiyama, Prog. Part. Nucl. Phys. **120**, 103868 (2021), arXiv:2010.07592 [hep-ph].

[20] T. Hyodo, Int. J. Mod. Phys. A **28**, 1330045 (2013), arXiv:1310.1176 [hep-ph].

[21] T. Kinugawa and T. Hyodo, Eur. Phys. J. A **61**, no.7, 154 (2025), arXiv:2411.12285 [hep-ph].

[22] 兵藤哲雄, 日本物理学会誌「最近の研究から」 第 75 巻第 8 号 478 (2020). `https://www.jstage.jst.go.jp/article/butsuri/75/8/75_478/_article/-char/ja/`

[23] 兵藤哲雄, 「数理科学」Vol.63-2, pp.28-35, サイエンス社, 2025. `https://www.rcnp.osaka-u.ac.jp/~hyodo/jp.html#jp8`

[24] 石坂 智, 小川 朋宏, 河内 亮周, 木村 元, 林 正人, 「量子情報科学入門」 第 2 版 (共立出版, 2024)

[25] Michael A. Nielsen, Isaac L. Chuang 「Quantum Computation and Quantum Information: 10th Anniversary Edition」 (Cambridge University Press, 2010).

[26] C. E. P. Robin and M. J. Savage, arXiv:2604.26376 [quant-ph].

[27] G. Gamow, Z. Phys. **51**, 204 (1928).

[28] H.M. Nussenzveig, Nucl. Phys. **11**, 499 (1959).

[29] T. Hyodo, Phys. Rev. Lett. **111**, 132002 (2013), arXiv:1305.1999 [hep-ph].

[30] T. Kinugawa and T. Hyodo, arXiv:2403.12635 [hep-ph].

[31] N. Hatano, K. Sasada, H. Nakamura, and T. Petrosky, Prog. Theor. Phys. **119**, 187 (2008), arXiv:0705.1388 [quant-ph].

[32] F.-K. Guo, X.-H. Liu, and S. Sakai, Prog. Part. Nucl. Phys. **112**, 103757 (2020), arXiv:1912.07030 [hep-ph].

[33] L. Castillejo, R. H. Dalitz, and F. J. Dyson, Phys. Rev. **101**, 453 (1956).

[34] Y. Kamiya and T. Hyodo, Phys. Rev. C **93**, 035203 (2016), arXiv:1509.00146 [hep-ph].

[35] Y. Kamiya and T. Hyodo, PTEP **2017**, 023 (2017), arXiv:1607.01899 [hep-ph].

[36] H. Feshbach, Ann. Phys. **5**, 357 (1958).

[37] H. Feshbach, Ann. Phys. **19**, 287 (1962).

[38] S. Inouye *et al.*, Nature (London) **392**, 151 (1998).

[39] A. Moerdijk, B. Verhaar, and A. Axelsson, Phys. Rev. A **51**, 4852 (1995).

[40] W. Heisenberg and H. Euler, Z. Phys. **98**, 714 (1936), physics/0605038.

[41] S. Weinberg, Physica A **96**, 327 (1979).

[42] S. Scherer and M. R. Schindler, *A Primer for Chiral Perturbation Theory* volume 830 (Springer, Berlin, 2012).

[43] E. Braaten, M. Kusunoki, and D. Zhang, Annals Phys. **323**, 1770 (2008), arXiv:0709.0499 [cond-mat.other].

[44] E. Braaten and H.-W. Hammer, Phys. Rept. **428**, 259 (2006), cond-mat/0410417.

[45] S. Weinberg, Phys. Rev. **137**, B672 (1965).

[46] T. Kinugawa and T. Hyodo, Phys. Rev. C **106**, 015205 (2022), arXiv:2205.08470 [hep-ph].

[47] K. Miyahara, T. Hyodo, and W. Weise, Phys. Rev. C **98**, 025201 (2018), arXiv:1804.08269 [nucl-th].

[48] F. Aceti, L. Dai, L. Geng, E. Oset, and Y. Zhang, Eur. Phys. J. A **50**, 57 (2014), arXiv:1301.2554 [hep-ph].

[49] Z.-H. Guo and J. A. Oller, Phys. Rev. D **93**, 096001 (2016), arXiv:1508.06400 [hep-ph].

[50] I. Matuschek, V. Baru, F. K. Guo and C. Hanhart, Eur. Phys. J. A **57**, no.3, 101 (2021), arXiv:2007.05329 [hep-ph].

[51] Y. Ikeda, T. Hyodo, and W. Weise, Phys. Lett. B **706**, 63 (2011), arXiv:1109.3005 [nucl-th].

[52] Y. Ikeda, T. Hyodo, and W. Weise, Nucl. Phys. A **881**, 98 (2012), arXiv:1201.6549 [nucl-th].

[53] S. Hill and W. K. Wootters, Phys. Rev. Lett. **78**, 5022 (1997), quant-ph/9703041.

[54] W. K. Wootters, Phys. Rev. Lett. **80**, 2245 (1998), quant-ph/9709029.

[55] A. Einstein, B. Podolsky and N. Rosen, Phys. Rev. **47**, 777-780 (1935).

[56] J. F. Clauser, M. A. Horne, A. Shimony and R. A. Holt, Phys. Rev. Lett. **23**, 880-884 (1969).

[57] J. S. Bell, Physics **1**, 195-200 (1964).

[58] S. J. Freedman and J. F. Clauser, Phys. Rev. Lett. **28**, 938-941 (1972).

[59] H. Sakai, et al., Phys. Rev. Lett. **97**, 150405 (2006).

[60] P. Naidon and S. Endo, Rept. Prog. Phys. **80**, 056001 (2017), arXiv:1610.09805 [quant-ph].

[61] P. Zanardi, C. Zalka, and L. Faoro, Phys. Rev. A **62**, 030301 (2000), quant-ph/0005031.

[62] I. Low and T. Mehen, Phys. Rev. D **104**, 074014 (2021), arXiv:2104.10835 [hep-th].

[63] Q. Liu, I. Low, and T. Mehen, Phys. Rev. C **107**, 025204 (2023), arXiv:2210.12085 [quant-ph].

[64] M. L. Wagman *et al.*, Phys. Rev. D **96**, 114510 (2017), arXiv:1706.06550 [hep-lat].

[65] T.-R. Hu, K. Sone, F.-K. Guo, T. Hyodo, and I. Low, Phys. Rev. Res. **7**, 043306 (2025), arXiv:2506.08960 [hep-ph].

[66] S. Gongyo *et al.*, Phys. Rev. Lett. **120**, 212001 (2018), arXiv:1709.00654 [hep-lat].

Number: Name:

Exercise 1 (deadline: April 28, 2026)

1) Consider one-dimensional quantum mechanics defined on $x \in [0, L]$. For $E > 0$, find the eigenfunctions $\phi_n(x)$ that satisfy the free Schrödinger equation with boundary conditions $\phi(0) = \phi(L) = 0$, and express them using an integer n:

$$-\frac{1}{2\mu}\frac{d^2}{dx^2}\phi(x) = E\phi(x).$$

2) For the eigenfunctions $\{\phi_n\}$, show that the momentum operator $p = -i\,d/dx$ is Hermitian, namely,

$$\int_0^L \phi_n^*(x) p \phi_m(x) dx = \int_0^L [p\phi_n(x)]^* \phi_m(x) dx.$$

3) For the eigenfunctions $\{\phi_n\}$, examine whether the operator p^3 is Hermitian (pay attention to boundary terms).

Number: Name:

Exercise 2 (deadline: May 12, 2026)

1) Derive the partial wave cross section $\sigma_l(E)$ in Eq. (41) by expressing the scattering amplitude $f_\ell(E)$ in terms of the phase shift $\delta_\ell(E)$.

2) Prove the following optical theorem:

$$\mathrm{Im}\, f(E, \theta = 0) = \frac{p}{4\pi}\sigma(E).$$

Number: Name:

Exercise 3 (deadline: May 26, 10:30 am, 2026)

1) Consider a perturbative solution of the pole condition (101). Let $E^{(n)}$ denote the nth-order contribution in $\hat{V}_t$ (or equivalently in $F(\boldsymbol{q})$) to the eigenenergy E, and expand the eigenenergy as

$$E = E^{(0)} + E^{(2)} + E^{(4)} + \cdots .$$

From Eq. (102), we have

$$E^{(0)} = \epsilon_0.$$

Because $\hat{V}_t$ is off-diagonal, there are no odd-order contributions to the energy E. Substituting this expansion into the self-energy $\Sigma(E)$, show that $E^{(2)} = \Sigma(\epsilon_0)$.
2) For $F(\boldsymbol{q}) = F(q^2)$ (i.e., spherically symmetric, depending only on q^2) and $\epsilon_0 > 0$, evaluate the imaginary part of E in the perturbative approximation $E = \epsilon_0 + \Sigma(\epsilon_0)$. Assume that $F(q^2)$ vanishes sufficiently rapidly as $|q^2| \to \infty$.

Number: Name:

Exercise 4 (no submission required)

1) Derive the expression for the scattering amiplitude in Eq. (117) from the Lippmann-Schwinger equation (116).

Number: Name:

Exercise 5 (deadline: June 23, 10:30 am, 2026)

1) Show the action of the Hadamard gate in Eq. (178).

2) Verify $|\uparrow\rangle\langle+| + |\downarrow\rangle\langle-| = H$ using the matrix representation.

3) Express $H\,|{+i}\rangle$ in terms of $|{-i}\rangle$.

Number: Name:

Exercise 6 (deadline: June 30, 10:30 am, 2026)

1) Derive the expression for the reduced density matrix in Eq. (223).

2) Derive the expression for the concurrence in Eq. (230). Here, $|\Psi^*\rangle = K|\Psi\rangle$ denotes the column vector whose components are the complex conjugates of those of $|\Psi\rangle$.

3) Derive the expression for the von Neumann entropy in Eq. (231).

4) Derive the expressions for the linear entropy in Eq. (232).

Number: Name:

Exercise 7 (no submission required)

1) Show that the equalities in the purity inequality (249) are satisfied for the probability distributions given in Eq. (250).

2) Show that the Bell state in the y basis,

$$\frac{|{+i}+i\rangle + |{-i}-i\rangle}{\sqrt{2}} = \frac{|{+i}\rangle \otimes |{+i}\rangle + |{-i}\rangle \otimes |{-i}\rangle}{\sqrt{2}}$$

is identical to $|\Phi^-\rangle$.

Number: Name:

Exercise 8 (no submission required)

1) We would like to reproduce the quantum-mechanical result in Eq. (281) using a hidden variable theory. Assume that the hidden variable is discrete, $i = 1, 2, 3, 4$, and define the probability distribution and the expectation value by

$$p_i = \rho(i), \qquad \sum_{i=1}^{4} p_i = 1, \qquad C(\boldsymbol{n}, \boldsymbol{m})_{\mathrm{HV}} = -\sum_{i=1}^{4} p_i N(\boldsymbol{n}, i) N(\boldsymbol{m}, i),$$

where the relation in Eq. (286) has been used. For each value of i, let

$$\begin{aligned} &N(\boldsymbol{n}, 1) = +1, \qquad N(\boldsymbol{m}, 1) = +1, \qquad N(\boldsymbol{n}, 2) = +1, \qquad N(\boldsymbol{m}, 2) = -1, \\ &N(\boldsymbol{n}, 3) = -1, \qquad N(\boldsymbol{m}, 3) = +1, \qquad N(\boldsymbol{n}, 4) = -1, \qquad N(\boldsymbol{m}, 4) = -1. \end{aligned}$$

This assignment satisfies the marginal distribution condition (277). Give one example of $\{p_i\}$ that reproduces Eq. (281).

2) Consider a continuous hidden variable $\lambda \in [0, 1]$ with a uniform distribution, $\rho(\lambda) = 1$. Choose

$$N(\boldsymbol{n}, \lambda) = \begin{cases} +1, & 0 \le \lambda < \frac{1}{2}, \\ -1, & \frac{1}{2} \le \lambda \le 1. \end{cases}$$

This choice satisfies the marginal distribution condition (277). Give one example of $N(\boldsymbol{m}, \lambda)$ that reproduces

$$C(\boldsymbol{n}, \boldsymbol{m})_{\mathrm{HV}} = -\int d\lambda\, \rho(\lambda) N(\boldsymbol{n}, \lambda) N(\boldsymbol{m}, \lambda) = -\cos\theta.$$

Number: Name:

Exercise 9 (deadline: July 21, 10:30 am, 2026)

1) Express $\boldsymbol{\sigma}_A \cdot \boldsymbol{\sigma}_B$ in terms of Kronecker products and derive the matrix representation in Eq. (308).

2) Using the matrix representation of $\boldsymbol{\sigma}_A \cdot \boldsymbol{\sigma}_B$, show that

$$\boldsymbol{\sigma}_A \cdot \boldsymbol{\sigma}_B \left|\Psi^-\right\rangle = -3 \left|\Psi^-\right\rangle , \quad \boldsymbol{\sigma}_A \cdot \boldsymbol{\sigma}_B \left|\Psi^+\right\rangle = +1 \left|\Psi^+\right\rangle .$$

3) Derive the actions of CNOT in Eq. (314).

Number: Name:

Exercise 10 (no submission required)

1) Derive the expression for the S-matrix in Eq. (344).

2) Derive the expressions for $E(U)$ and U in Eq. (346) with $\beta_1 = \beta_2 = \beta_3 = \beta$.

Number: Name:

Exercise 11 (no submission required)

1) Derive the expressions for s_x and s_y for a spin-3/2 particle given in Eq. (376). Recall the properties of the ladder operators

$$s_\pm = s_x \pm i s_y, \quad s_\pm |s,m\rangle = \sqrt{s(s+1) - m(m\pm 1)}\, |s, m\pm 1\rangle\,,$$

with

$$|\Uparrow\rangle = |3/2, 3/2\rangle\,, \quad |\uparrow\rangle = |3/2, 1/2\rangle\,, \quad |\downarrow\rangle = |3/2, -1/2\rangle\,, \quad |\Downarrow\rangle = |3/2, -3/2\rangle\,.$$

2) Derive the projection operator $\mathcal{J}_0$ in Eq. (383) using the following procedure. The operator

$$X = \boldsymbol{s}_A \cdot \boldsymbol{s}_B$$

for two spin-3/2 particles has the eigenvalues

$$x_S = \frac{1}{2}\left[S(S+1) - \frac{15}{2}\right],$$

for the total-spin states with $S = 0, 1, 2, 3$. Since X has four distinct eigenvalues, it satisfies the minimal polynomial

$$(X - x_0)(X - x_1)(X - x_2)(X - x_3) = 0.$$

Hence every power X^n with $n \geq 4$ can be reduced to a linear combination of $1, X, X^2$, and X^3. Therefore, each projection operator can be written as a cubic polynomial in X:

$$\mathcal{J}_0 = a + bX + cX^2 + dX^3,$$

Determine the coefficients a, b, c, and d.
